Analysis of mode of action of antiarrhythmics
in isolated cardiac preparations:

The ultrarapid delayed rectifier K^+ current as potential target for treatment of human atrial fibrillation

PhD Thesis

Ottó Hála, Dr.Univ.Med.Biol

Department of Pharmacology and Pharmacotherapy

Faculty of Medicine

Albert Szent-Györgyi Medical and Pharmaceutical Center
University of Szeged

Szeged, Hungary

2003

CONTENTS

LIST OF PUBLICATIONS RELATED TO THE SUBJECT OF THE THESIS

Papers

I. **Hála O**, Németh M, Varró A, Papp JGy. Electrophysiologic effects of detajmium on isolated dog cardiac ventricular Purkinje fibers. *J Cardiovasc Pharmacol.* 1994; 24:559-565.
Impact factor: 1.680 (1994), 1.553(2001)

II. Németh M, Virág L, **Hála O**, Varró A, Kovács G, Thormälen D, Papp JGy. The cellular electrophysiological effects of tedisamil in human atrial and ventricular fibers. Cardiovasc Res. 1996; 31: 246-248.
Impact factor: 3.268 (1996), 4.552(2001)

III. Németh M, Varró A, Virág L, **Hála O**, Thormälen D, Papp JGy. Frequency-dependent cardiac effects of tedisamil: comparison with quinidine and sotalol. *J Cardiovasc Pharmacol Therapeut.* 1997; 2(4):273-284.
Impact factor: -

IV. Dobrev D, Graf EM, Wettwer E, Himmel HM, **Hála O**, Doerfel C, Christ T, Schüler S, Ravens U. Molecular basis of downregulation of G-protein-coupled inward rectifying K^+ current ($I_{K,ACh}$) in chronic human atrial fibrillation: Decrease in GIRK4 mRNA correlates with reduced $I_{K,ACh}$ and muscarinic receptor-mediated shortening of action potentials. *Circulation.* 2001; 104:2551-2557.
Impact factor: 10.517(2001)

Abstracts

V. **Hála O**, Papp JGy: Effective Algorithm for on-line analysis of electrophysiological signals recorded from isolated cardiac preparations. in Murray A, Arzbaecher R (eds) : *Computers in cardiology*, Vienna 1995; IEEE 95CH35874: 413-415.

VI. Dobrev D, Graf EM, Wettwer E, Himmel HM, **Hála O**, Doerfel C, Christ T, Schüler S, Ravens U. Molecular basis of $I_{K,ACh}$ downregulation in chronic atrial fibrillation. Decrease in GIRK4 mRNA correlates with reduced muscarinic receptor-mediated shortening of action potential. *Circulation.* 2001; 104(17 Suppl II): P642.

VII. **Hála O**, Wettwer E, Dobrev D, Christ T, Papp JGy, Ravens U. Selective outward current block with low concentration of 4-aminopyridine reveals a prominent role of IK_{ur} in determining the action potential plateau shape of human atrial tissue. *Circulation.* 2001; 104(17 Suppl II): P1328.

INTRODUCTION

Atrial fibrillation in general

Atrial fibrillation is one of the most common irregular heart rhythms. It affects more than 2.2 million people and more than 160,000 new cases of atrial fibrillation are diagnosed in the United States each year. The impulse rate through the atria can range from 300 to 600 beats per minute. Fortunately, the atrioventricular node limits the number of impulses that go to the ventricles. The resulting heart beat becomes irregular, ranging from about 50 to 150 beats per minute[1]. In 90% of the cases, atrial fibrillation is secondary to some cardiovascular or related chronic disease such as hypertension, coronary artery disease, valve disease, chronic lung disease, heart failure, chardiomyopathy, congenital heart disease, a pulmonary embolism, hyperthyroidism or pericarditis. It frequently evolves after open chest cardiac surgery. In 10% of the cases atrial fibrillation develops as a direct consequence of alcohol abuse, excessive caffein use, stress, intoxication from taking illicit drugs, electrolite or metabolic imbalances, or severe infection. In some cases there may be no identifiable cause. It could be that hereditary channelopathies are responsible for this type of atrial fibrillation of obscure origin[2]. The risk of atrial fibrillation increases with age, especially after sixty[3], and is clearly dependent on the gender and ethnicity[4,5]. At present, atrial fibrillation is regarded as a dangerous disease. Because in atrial fibrillation the heart beats rapidly and irregularly, blood flow through the atria is not satisfactory. This makes the blood more likely to clot. If a clot is pumped out of the heart it can travel to the brain, resulting in a stroke[6,7]. People with atrial fibrillation are 5 to 7 times more likely to have a stroke than the average person. A clot can also travel to other organs (kidneys, heart, intestines) and damage them. In 20 to 30% of cases atrial fibrillation impairs the pumping ability of the heart, precipitating or inducing heart failure. Chronic atrial fibrillation is associated with an increased risk of death[3].

Chronic atrial fibrillation is known to be accompanied by many changes both at the tissue and cardiomyocyte level. From an electrophysiological point of view the most typical changes are those associated with the restitutional properties and form of the action potential. Novel pharmacological interventions suitable for long-term medication of the disease, as well can not be contrived without a better understanding of the processes behind electrophysiological mechanisms.

The normal atrial action potential

The "spike-and-dome" shape of the normal human atrial trabecular action potential can be characterized by a steep early repolarization (2-5 ms APD_{20}), a low plateau potential (-25 -30 mV) and a slow late depolarization (300 - 400 ms APD_{90})[8]. The speed of the fast

depolarization (V_{max}) of the atrial action potential is comparable to the ventricular action potential, and is generally between 190 and 400 V/s[9,73,83,85].

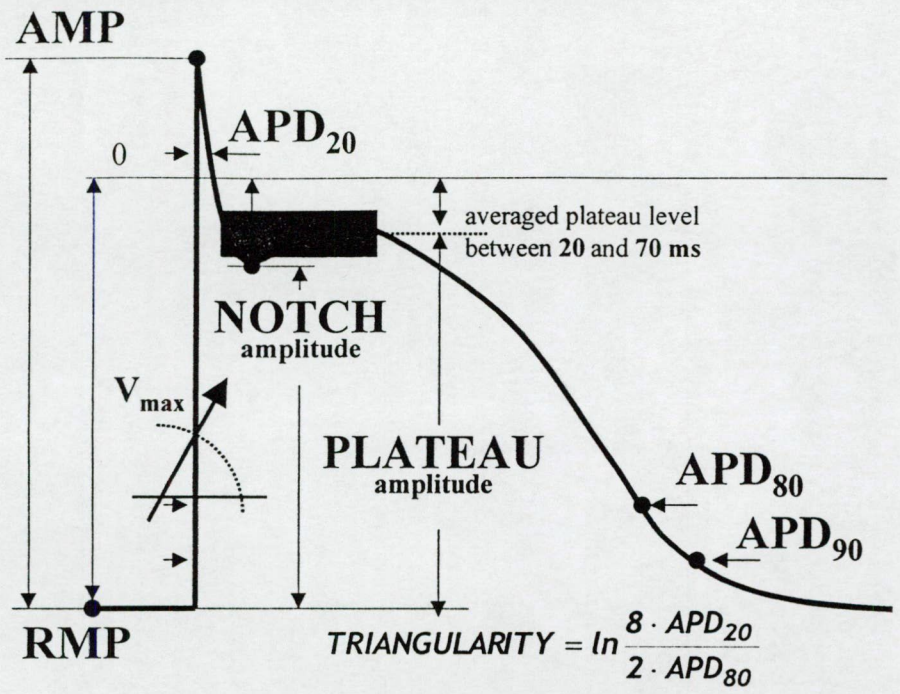

FIGURE 1

The normal human action potenial and its electrophysiological parameters

The characteristic parameters of atrial action potentials are the same for all excitable tissues. They can be characterized by a resting potential (RMP), amplitude of the action potential (AMP) and the action potential duration at different repolarization levels (APD_{10-90}). In order to characterize the "spike-and-dome" shape of action potentials, the relative or absolute values of notch and plateau amplitudes are used. Taking into account the fact that the shape of atrial action potentials may vary considerably owing to the effects of physiological pathophysiological processes and drugs, and also that the shape of action potentials and the liability of atrial tissue to fibrillate are strongly connected, the proportionality between APD_{20} and APD_{80} (TRIANGULARITY) is also a useful parameter[10] (**Fig 1**) for classifying the action potential.

Main ionic currents and their role in electrical activity of the atrial myocardium

The form of the atrial action potential arises from a complex interplay between different ionic currents. Early fast depolarization is brought about by fast Na^+ channels[11] (I_{Na}), as is the case in every excitable tissue. The contraction is triggered by Ca^{2+} entering the cells through the slow Ca^{2+} channels[12] (ICa_L). When determining the intracellular Ca^{2+} contents ($[Ca^{2+}]_i$) of intracellular Ca^{2+} stores other Ca^{2+} channels are also important. These are the T-type Ca^{2+} channel (ICa_T) operating in the resting potential range[13], the tetrodotoxine-sensitive Ca^{2+}

channel[14] (ICa_{TTX}), and as some yet undetermined Ca^{2+} channels that carry the so-called "capacitive" Ca^{2+} currents[15]. It is known that there are two extrusion mechanisms for removing Ca^{2+} from the cell. These are the Na^{+}-Ca^{2+} exchanger[16] ($NaCa_{Ex}$) which uses the electrochemical gradient of Na^{+} and the sarcolemmal Ca^{2+} pump[17] ($SRCa_{pmp}$). As to what extent these two mechanisms are responsible for maintaining normal intracellular Ca^{2+} concentrations under various physiological and pathophysiological conditions is still only partially understood. The direction of Na^{+}-Ca^{2+} exchange varies during the action potential phases. At potentials corresponding to the plateau of the action potential Na^{+} is extruded from the cell and Ca^{2+} is transported into it. The Na^{+}-Ca^{2+} exchanger reaches its maximal activity around the peak of the plateau of the atrial action potential, thereby influencing the time course of repolarization[18]. Early fast repolarization is brought about by a transient outward K^{+} current[19,20,21] (I_{to}) and by the atrium-specific ultrarapid delayed rectifying K^{+} current[22,] (IK_{ur}).

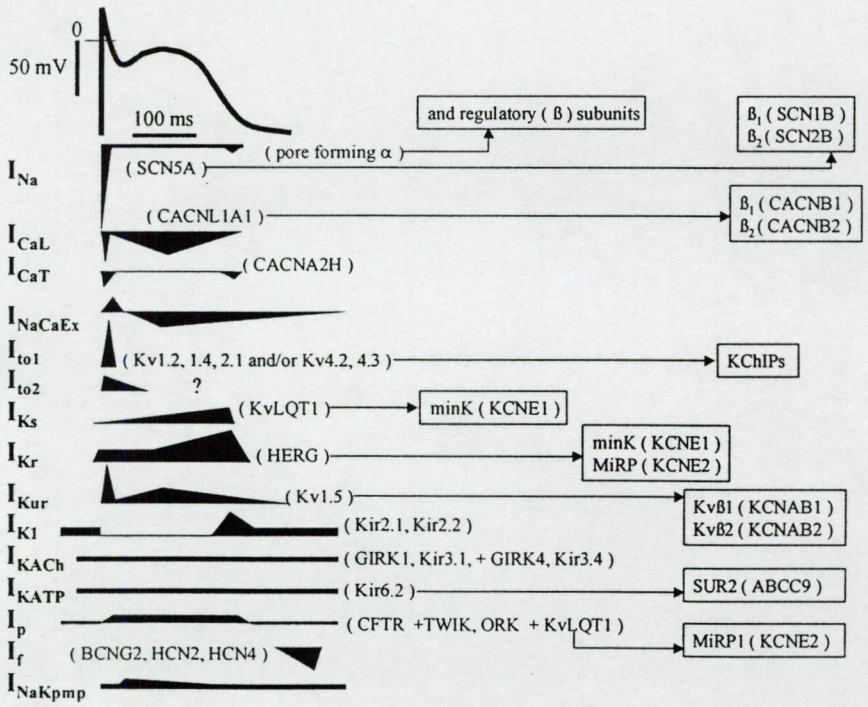

FIGURE 2

Ionic currents and the gene correlates of the pore forming and regulatory subunits in the human atrial myocardium[23,24,32]

In atrial tabecular muscles, IK_{ur} is one of the most important repolarizing currents. Atrial tabecular muscle contains conventional slow and fast K^{+} channels similar to other myocardial muscles that can be activated with normal action potential configurations, as well. The most important of them are the rapid and slow delayed rectifier K^{+} currents (IK_s and IK_r), which become activated during the action potential plateau[25,26]. If a repolarization level of 50-60 % is exceeded the inward rectifier K^{+} channel (IK_1) is activated and the outward current flowing

through this channel further assists the membrane to return to the resting potential[27,28]. The activity of inward rectifier K^+ channels are not important in overshooting or in the plateau domain of the action potentials. The shift in ionic concentrations through action potentials are restored by the Na^+-K^+ pump ($INaK_{pmp}$). The pump is electrogenic and takes part in the final shaping of the action potentials[29]. Atrial tissue contains other ionic channels too, the two most important being the acethycholine-sensitive (IK_{ACh}) and ATP-sensitive K^+ channels (IK_{ATP})[30,31]. During the plateau phase a sustained outward current is also activated (I_p). However, this macroscopic current is the result of more than one primary channel function with different kinetics and varying ion-specificity[32]. In the tissue of the right atrium under normal physiological conditions a channel responsible for the pacemaker current (I_f) can also be observed[33]. The membrane density of this channel is not yet known. To complicate the picture it should be noted that the presence of ionic channels or channel proteins does not necessarily mean that these channels are functional. Most likely each channel can be coupled to one or more regulatory protein. A given regulatory protein can modify the behaviour of more ionic channels. Ionic channels can be coupled to structural proteins available intra- or extracellularly, which can also modify their kinetic parameters[32] (**Fig 2**). In theory one could conceive of a situation where the results of measurements of currents may be the same although the detailed composition of channels and regulatory proteins are quite different. The variation of the channel composition and the up- and down–regulation of some channels can produce significant changes in the shape of the action potentials (electrical remodelling) and, as a consequence, changes in the restitution parameters of the action potentials. The unfavourable changes of the restitution parameters of the action potentials are considered today to be the most important factors in the onset and continuation of atrial fibrillation[34,35,36].

Electrical remodelling and its importance in the perpetuation of atrial fibrillation

The elevated atrial frequency may be a consequence of automacy or reentry which eventually leads to the perpetuation of atrial tachycardy, to atrial flutter and to chronic atrial fibrillation[37,38]. It seems that the regularity and organization of electrical activity, by following the tachycardy-atrial flutter-atrial fibrillation sequence[39], gradually shifts from temporally organized patterns (sinus-rhythm and tachycardy) to spatially-organized patterns (atrial flutter and chronic atrial fibrillation). The key characteristic of atrial fibrillation is the appearance of spatial independence and multiplication of time scales[40]. Whatever the reason for it the consequence of rhythm enhancement will undoubtedly be a steady increase in intracellular Ca^{2+} concentrations[17,18,41,42] (**Fig 3**).

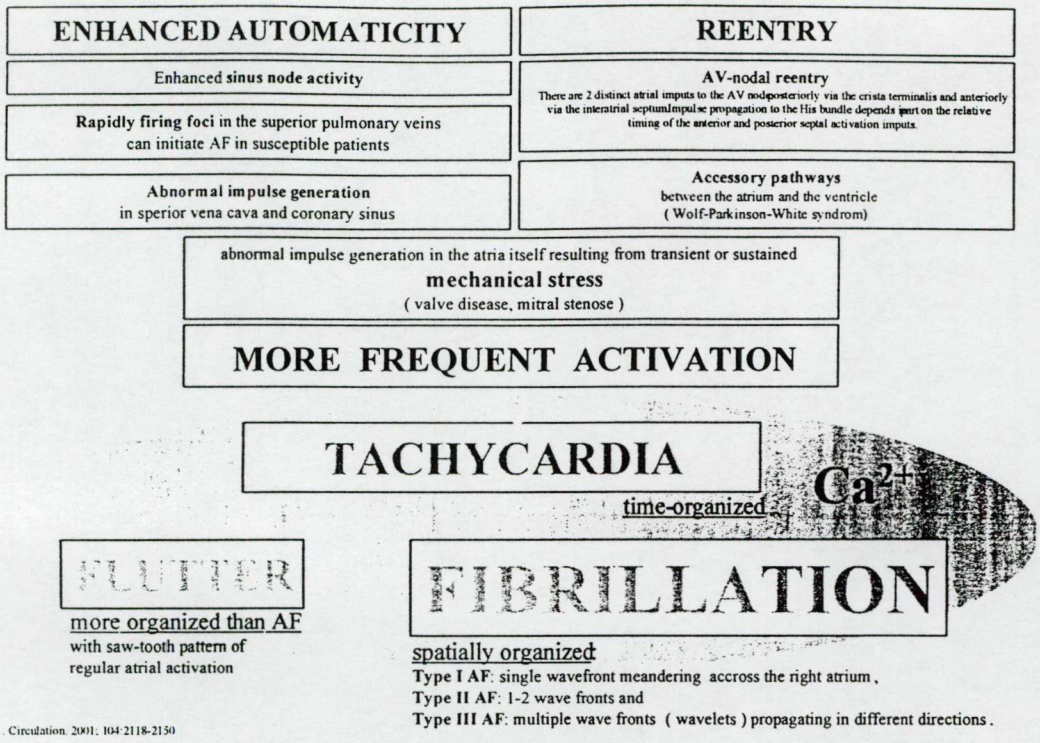

FIGURE 3

More frequent activation of atrial myocytes leads to an increase in the overall intracellular Ca^{2+} concentration

Alongside these changes, the atrial action potential becomes triangular in form and the mechanical activity gets reduced. It is well known that in fibrillating human myocardium the density of L-type Ca^{2+} channels is low. Data on the alterations of density of fast Na^{+} channels are contradictory. In fibrillating atrial myocardium the density of transient outward K^{+} channels is also low. The densities of the IK_{ACh} and IK_{ATP} channels, as well as the amount of calsequestrin in the sarcoplasmic reticulum are down-regulated too. However, the I_f density in the sarcolemma and number of IP_3-sensitive Ca^{2+}-release receptors in intracellular reticular membranes are upregulated. The densities of other repolarizing K^{+} channels are also altered by chronic atrial fibrillation. Moreover IK_{ur}, IK_s and IK_r are unchanged or down-regulated, while IK_1 is either elevated or decreased[41,43] (**Fig 4**).

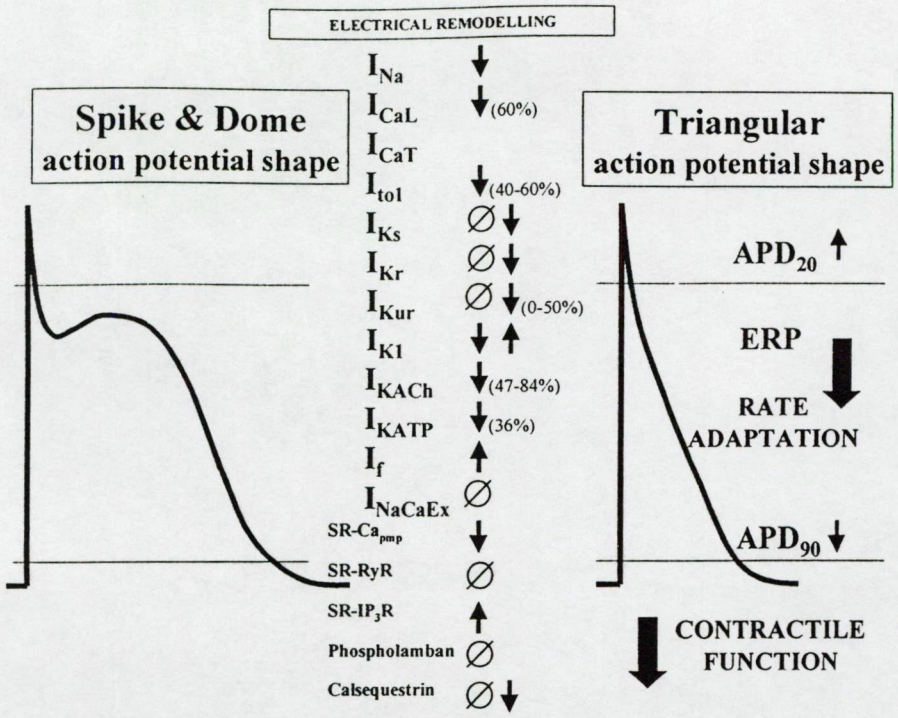

FIGURE 4

Changes in densities of ionic channels and Ca^{2+} handling proteins and the consequences on the electrical and mechanical activity in chronic atrial fibrillation

Combining the results of experiments on human preparations and animal fibrillation models, what seems to be an overall response of the mammalian myocardium to the atrial fibrillation is the down-regulation of Ca^{2+} channels together with that of repolarizing K^+ currents operating in voltage domains of these Ca^{2+}-channels[44] (**Fig 5**). It is worth noting, that there is no perfect experimental model for atrial fibrillation. This is partly because distinct species expressing though similar channel composition may utilize considerably different mechanisms to minimize detrimental cellular effects of the atrial fibrillation. Diverse changes in the IK_s, IK_r and IK_1 densities may reflect the fact that "sterile" atrial fibrillation in humans is relatively rare and atrial fibrillation is more often a consequence of other disorders[45,46]. To make a precise distinction between original and secondary processes in this respect is still quite impossible.

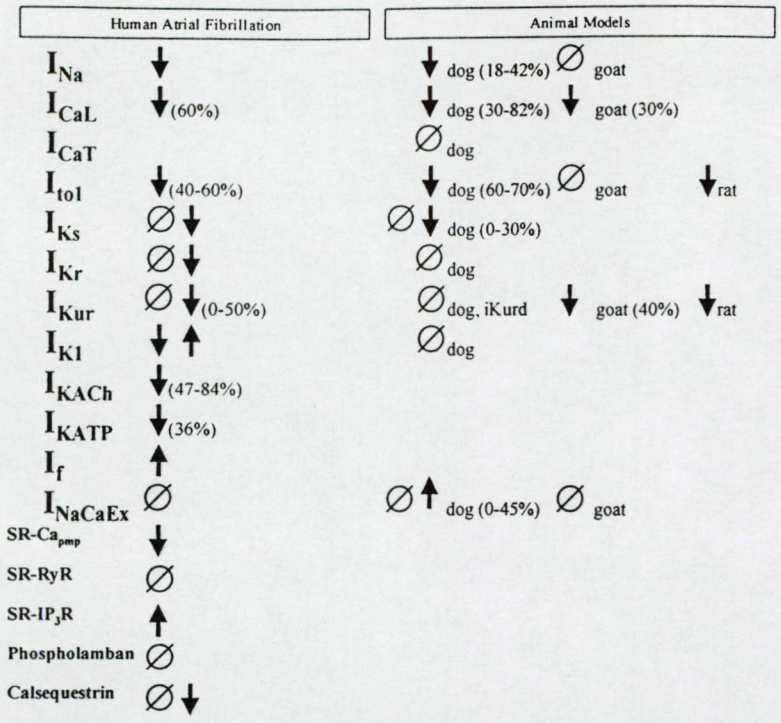

FIGURE 5

Remodelling in human atrial fibrillation and animal fibrillation models

Diversity of the trabecular action potential forms

Our results obtained from analyzing the incidence of the different action potential forms in isolated right atrial preparations from "healthy" subjects or from patients with atrial fibrillation also highlight the importance of other pathological processes which may trigger the disease. The frequency of triangular action potential forms was 24% in atrial trabeculae from "non-fibrillating" patients. In atrial fibrillation the triangular action potential form is thought to be unexceptionally common. In our current experiments, however, the typical triangular shape was characteristic only in 69% of diseased patients (**Fig 6**). This means that atrial fibrillation induces remodelling (i.e changes in densities of ionic channels and in the shape of the atrial action potentials), but remodelling can occur for other reasons too[45,46]. In the latter case atrial fibrillation is a consequence rather than a cause. The seemingly attractive statement "atrial fibrillation begets atrial fibrillation"[47] should perhaps be amended to "remodelling begets atrial fibrillation - and vice versa - atrial fibrillation begets remodelling". No doubt the mechanism for atrial fibrillation is a *circulus vitiosus* which has two entry points.

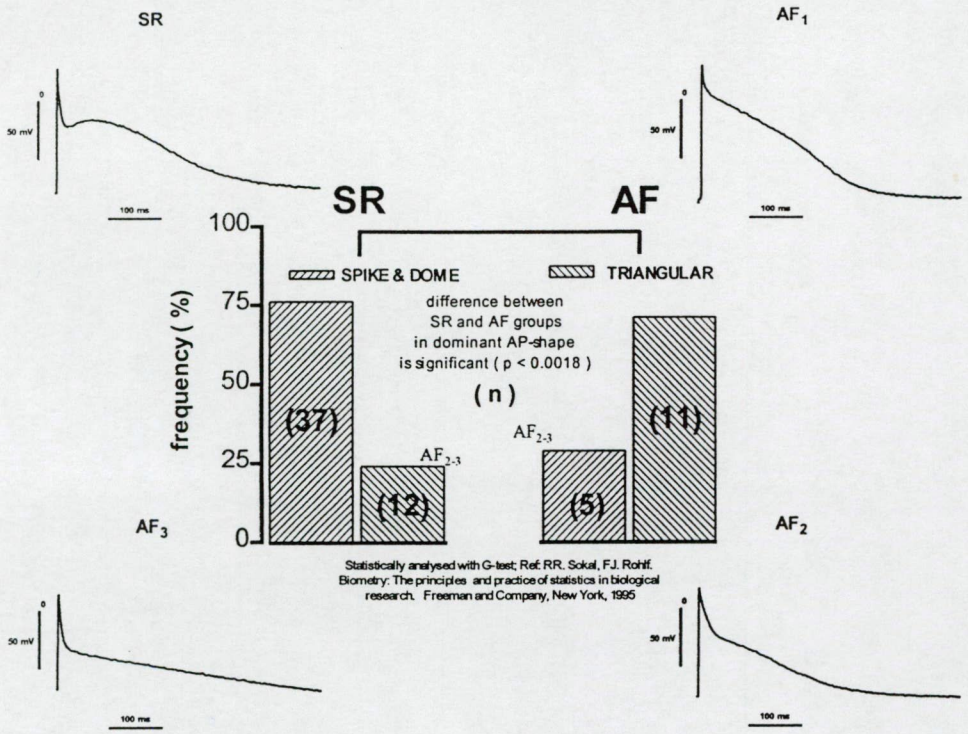

FIGURE 6

The occurence of fibrillating (triangular) action potential forms in human right atrial trabeculae obtained from patients either with sinus-rhythm (SR) or with diagnosed atrial fibrillation (AF)

Problems with drugs presently used in the treatment of atrial fibrillation

Many medications for the treatment of atrial fibrillation are available at present[48,49,50]. These drugs include quinidine, procainamide, disopyramine, propafenone, flecainide, sotalol[51], dofetilide, ibutilide[52], tedisamil, azimilide[53,54] and amiodarone[55,56] (Class1 and 3 antiarrhythmics according to Vaughan-Williams[57,58,59]), beta-blockers such as carvediol or propranolol (Class 2) and non-dihydropyridine Ca-antagonists like verapamil[60,61] or diltiazem[62] (Class 4) or digoxin. The principal drawback about them all is that they are not organ specific enough (they also influence the ventricular functions). Their effectiveness is unsatisfactory in practice (they are effective only in 30-60% of the cases and this effectiveness may even decrease with time; most drugs have a 70% failure rate after one year) and many of them possess potentially serious side effects. Over the past decade various studies have demonstrated that long-lasting preventive administrations of Class1 antiarrhythmics should be avoided in patients who had heart failure, cardiac ischaemia or a previous myocardial infarction because of the enhanced propensity of proarrhythmia[63], which may increase the mortality rate. Pure Class 3 drugs like sotalol[64], ibutilide and dofetilide also

share this proarrhythmic feature; they show a high rate of incidence of torsade de pointes (reported values in studies vary from 1 to 4.8% for the Class 3 antiarrhythmics and from 2 to 8.8% for quinidine)[65].

IK_{ur} as a potential target in the treatment of atrial fibrillation

The discovery of IK_{ur} in the early 90s[66,67] gave a new impetus to the development of atrial specific antiarrhythmics. It was shown that this channel could selectively be blocked by micromolar 4-aminopyridine (4-AP) concentrations[26,68]. Although earlier experiments on the 4-AP effects in multicellular preparations could not demonstrate unambigous APD lengthening[69,70] (a noticeable sign of antiarrhythmic action of selective K^+ channel blockers), leading researchers have since begun to hold the view that 4-AP does indeed prolong the APD in both healthy and remodelled atrial myocytes[71] and the application of 4-AP or similar compounds should be the breakthrough in the treatment or prevention of atrial fibrillation of any type.

AIM OF THE PRESENT STUDY

The aim of the present study was to examine whether the effects of the 4-AP caused an IK_{ur} block on the action potential parameters in right atrial preparations obtained from healthy individuals and also from patients with chronic atrial fibrillation going back 3 months or more. Keeping in mind, that a preponderant number of the subjects get the first incidence of atrial fibrillation at the predominance of the parasympathetic tone, 4-AP experiments with complete muscarinergic (M2) receptor activation were also considered. The action potential restitution and modification by antiarrithmics is known to play a crucial role both in the pathomechanism and the antiarrhythmic therapy of rhythm disturbances. Hence we also intended to characterize 4-AP effects on the action potential restitution in atrial preparations of either type (i.e. "healthy" or "sinus-rhythm" and "fibrillating"). In order to verify the 4-AP–induced action potential effects and also to explore the IK_{ur} block–induced secondary changes in other important current entities of the atrial myocardium, we intended to develop an action potential model. It was also considered that, by revealing the exact interplay of ionic currents during the atrial action potential, new antiarrhythmic approaches might also be suggested. The mechanism of action of 4-AP was also compared with those of lidocaine, detajmium[83] and tedisamil[72 85].

METHODS

Human atrial preparations

Right atrial appendages were obtained from 49 patients with sinus-rhythm and 16 patients with chronic atrial fibrillation. There was a slight differences in sex, underlying heart disease and left atrial diameter between the two groups. Patients with atrial fibrillation were more frequently medicated with digitalis, Ca-antagonists of non-dyhydropyridine type and nitrates than sinus rhythm patients. However, verifying the differences statistically proved impossible in practice because of the low number of cases. The existence of such differences is well known and has also been demonstrated by us in other experiments [73].

Other types of cardiac preparations

In experiments for analyzing the effects of drugs on cardiac action potentials of other species, canine and rabbit preparations were also used. The concerning methodological details are published elsewhere[83,85,87].

Action potential recordings

About 25 min after the appendages had been removed the atrial trabeculae were prepared. Then the trabeculae were mounted onto the bottom of an organ bath perfused with oxigenated Tyrode's solution having a molar composition like that published elsewhere[73,87]. Before starting an experiment, the preparations were left to stabilize for 40 min. During this adaptation period and also throughout the whole experiment, the preparations were subjected to rectangular pulse stimuli at a driving rate of 1Hz. Transmebrane potentials were recorded via microelectrode impalement. When the preparations failed to function and action potentials could not be evoked even when exceptionally high stimulus intensities were applied, 1 μM carbachol was added to the bath. If the electrical activity was restored and carbachol could be removed without worsening of the transmebrane potential parameters (i.e. changes remained within 1% for 10 min after a 30 min long washout) the preparations were regarded as normal. Otherwise they were rejected.

Action potential restitution

The action potential restitution was established by using extra impulses at 1Hz basic cycle length. Extra impulses were delivered to the preparation after every tenth regular beat. The coupling time of extra impulses was alternatedly varied in a 3000 ms range following the effective refractory period.

Transmembrane potential parameters followed

In addition to the usual parameters (the resting potential: RMP, action potential amplitude: AMP, maximum rate of depolarization: V_{max}, action potential durations at different percentage values of repolarization: APD_x) parameters for the the action potential notch (NOTCH) and the action potential plateau (PLATEAU) were introduced. The action potential form was characterized by a triangularity parameter (TRIANGULARITY) calculated as the natural logarithm of the weighted APD_{20}/APD_{80} ratio. (**Fig 1**) Numeric values of the relevant parameters were obtained automatically from signals obtained via a program written by the author[83,87].

Drugs applied in this study

In the present work, detajmium, tedisamil, 4-aminopyridine (4-AP), carbachol and E-4031 were used. Small amounts of stock solutions were added directly to the organ bath. Concentration-response relationships were determined by applying (4-AP) cumulatively. In the case of E-4031, the solvent was dimethyl-sulfoxide (DMSO). To exclude unwanted solvent effects, single experiments were also carried out solely with DMSO. In these experiments DMSO did not alter the transmebrane potential when its volume-concentration remained below 0.2%. This DMSO concentration was never exceeded in our experiments. Incubation with each set 4-AP concentration lasted for 20-40 min. Lidocaine and carbachol effects were left to evolve for 15-30 min. The exposure to detajmium, tedisamil or E-4031 lasted for 30-50 min.

Statistical analysis

Drug effects were statistically verified with Student's t test for paired observations. In the case of the restitution curves one-way ANOVA and Bonferroni post tests were used for statistical evaluations. The results with E-4031 were statistically analyzed with one-way ANOVA and Dunn's test. The diversity of action potential forms in sinus rhythm and atrial fibrillation was statistically verified by applying the G-test. All the data obtained experimentally are expressed as means ±SE. Changes were regarded as significant when $p<0.05$.

Computer simulation

The human atrial action potential model was based on the research work of others[71,74,75,76,77,78,79,80,81]. It was written in the PASCAL language and was run in DOS mode on an 800 MHz IBM-clone PC with Pentium II processor. The maximum conductance values of ionic currents were taken from the literature. In order to get realistic action atrial potential forms most of them had to be readjusted. For numerical integration of the mebrane potential change caused by the instantaneous transmembrane currents a modified Euler-method was

applied[78]. Depending on the estimated error, the integration step was varied automatically between 0.001 and 1ms. Before recording a simulated action potential, ionic concentrations in different compartments were left to stabilize for 200 cycles. (APPENDIX: **Fig 23**, **TABLE 6-8**). All simulations had a steady-state driving rate of 1Hz[82].

RESULTS

4-aminopyridine concentration-respons curves at 1Hz rate in SR-preparations

In "healthy" atrial appendage preparations stimulated at a driving rate of 1Hz, 4-AP induced concentration dependent changes in action potential parameters, especially in those for the plateau phase and action potential durations at repolarization levels below 50%. Increasing 4-AP concentrations ranging from 0.3 to 100 μM elevated the height of the action potential plateau (control: -22.6 ±0.8 mV, 100μM 4AP: -2.8 ±1.9 mV, n=5) with an EC_{50} of 13μM. Besides the plateau elevation, the notch potential was moved to more positive values (control: -26.1 ±1.2 mV, 100 μM 4AP: -6.3 ±1.1 mV, EC_{50}: 16 μM) and the APD_{90} value was shortened (control: 293.7±15.1 ms, 100μM 4AP: 243.2±11.8 ms, EC_{50}: 7.3μM). Even when 100 μM or higher 4-AP concentrations have been applied, the effects could always be reversed in 30 min after the removal of the drug. (**Fig 7**). The lowest 4-AP concentrations inducing statistically verifiable plateau elevation seemed to be between 3 and 10 μM.

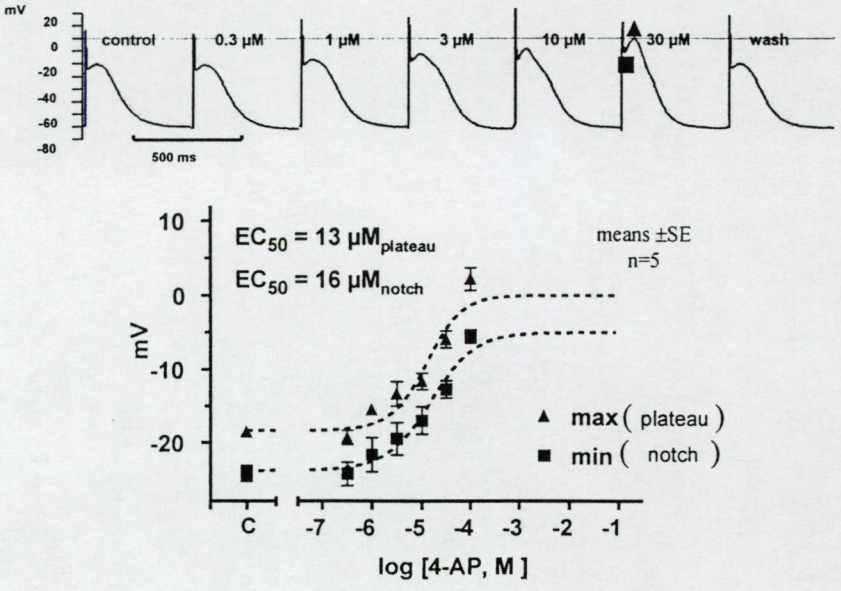

FIGURE 7

Human right atrial action potentials as affected by increasing 4-aminopyridine concentrations at 1 Hz steady-state driving rate

The effects of low 4-aminopyridine concentrations on the action potential parameters in right atrial trabecules obtained from patients with sinus rhythm

5μM of 4-AP significantly elevated the notch and plateau potentials from –31.7 ±4 to –21.8 ±4.8 and from –21.0 ±2.5 to –6.5 ±2.5 mV (n=16). At the same time, the APD_{80} and APD_{90} values were significantly shortened by 9 and 15% respectively (APD_{80}: 290.8 ±6.2 vs. 264 ±8.0 ms [$p < 0.010$] and APD_{90}: 413.6 ±10.4 vs. 350.0 ±10.1 ms [$p < 0.001$]). V_{max}, the action potential amplitude and APDs below 20% of repolarization did not change significantly. In the presence of 5 μM of 4-AP the sinus rhythm action potentials became noticeably more triangular (**TABLE 1**, **Fig 8A**).

TABLE 1

Effect of 5-μM 4-aminopyridine on the action potential parameters at a driving rate of 1Hz in human right atrial appendages obtained from patients with sinus-rhythm

	RMP (mV)	AMP (mV)	V_{max} (V/s)	APD_{20} (ms)	APD_{80} (ms)	APD_{90} (ms)	NOTCH (mV)		PLATEAU (mV)		TRIANGULARITY
							abs	**amp**	**abs**	**amp**	
control	-75.2 ±0.8	100.9 ±2.1	280.7 ±15.7	4.9 ±1.6	290.8 ±6.2	413.6 ±10.4	-31.7 ±4.0	43.5 ±4.3	-21.0 ±2.5	54.2 ±2.9	-3.2 ±0.22
+ 5μM 4-AP	-74.4 ±1.0 ★	100.0 ±2.3	267.3 ±15.7	12.1 ±4.8 ★	264.1 ±8.0 ★	350.0 ±10.1 ★	-21.8 ±4.8 ★	52.7 ±5.3 ★	-6.4 ±2.5 ★	68.0 ±3.1 ★	-2.4 ±0.31 ★

mens±SE, n = 15, ★: $p < 0.05$, **abs**: absolute values, **amp**: amplitude from RMP

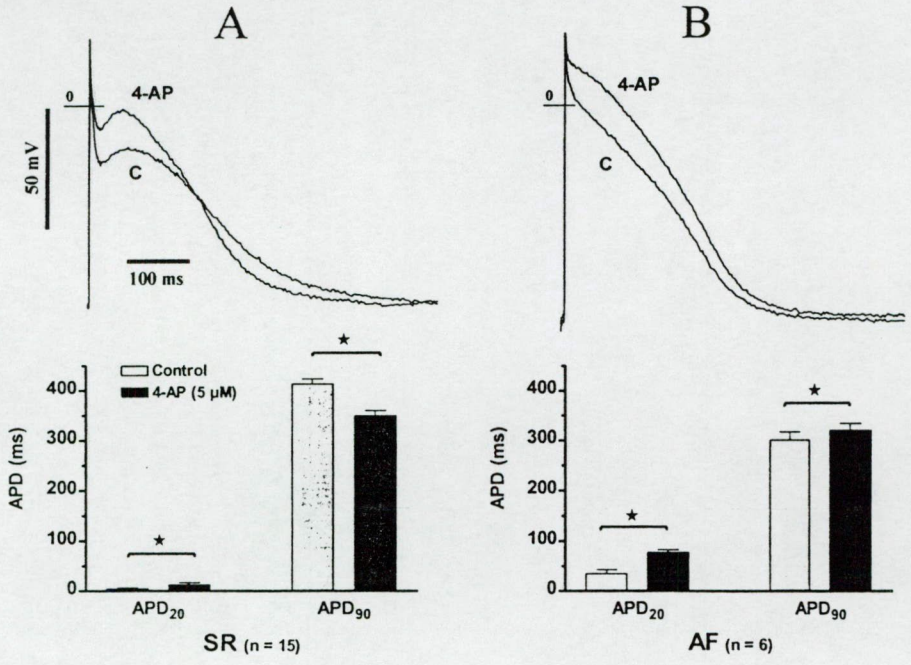

FIGURE 8

Human right atrial action potentials in sinus rhythm (A) and atrial fibrillation (B) as affected by 5 μM of 4-aminopyridine at a steady-state driving rate of 1Hz

The effects of 4-aminopyridine concentrations in atrial fibrillation

In trabeculae taken from patients with chronic atrial fibrillation, the action potential plateau runs routinely above 0 mV and the notch potential can not clearly be defined or its position in repolarization can vary quite considerably. 5 μM of 4-AP was able to further elevate this increased fibrillating action potential plateau by 15% (control: 0.36 ±3.3 mV, 4-AP: 12.4 ±2.5 mV; n =6 [$p< 0.01$]). The increase in the notch amplitude caused by the drug was also detectable but its true extent may be somewhat overestimated because the determination of this parameter is imprecise with highly triangular action potential forms. In contrast with sinus-rhythm preparations, the APD_{80} and APD_{90} values were lengthened by 5μM of 4-AP in "fibrillating" trabeculae (from 233.8 ±12.0 to 258.5 ±10.9 ms [$p<0.01$] and from 300.4 ±16.3 to 320.2 ±13.3 ms [$p<0.01$], respectively). The numerical value of the 4-AP-induced increase in the APD_{20} value (123%) could be solely attributed to drug-effects on the height of the action potential plateau. Neither V_{max} nor the resting potential and action potential amplitude were changed by 5 μM 4-AP in tabeculae from patients with atrial fibrillation. (**Fig 8B, TABLE 2**)

TABLE 2
Effect of 5-μM 4-aminopyridine on the action potential parameters in human right atrial appendages obtained from patients with chronic atrial fibrillation at driving rate of 1Hz

	RMP (mV)	AMP (mV)	V_{max} (V/s)	APD_{20} (ms)	APD_{80} (ms)	APD_{90} (ms)	NOTCH (mV)		PLATEAU (mV)		TRIANGULARITY
							abs	**amp**	**abs**	**amp**	
control	-79.7 ±2.7	106.5 ±3.4	291.0 ±28.2	34.8 ±8.6	233.8 ±12.0	300.4 ±16.3	-52.8 ±11.9	26.8 ±12.0	0.4 ±3.3	80.0 ±2.4	-0.71 ±0.28
+ 5μM 4-AP	-79.3 ±2.6	106.8 ±2.3	291.6 ±20.3	77.7 ±5.0 ★	258.5 ±10.9 ★	320.2 ±13.3 ★	-23.9 ±15.1 ★	55.4 ±15.8 ★	12.4 ±2.5 ★	91.8 ±1.6 ★	0.18 ±0.05 ★

mens±SE, n = 6, ★: $p < 0.05$, **abs**: absolute values, **amp**: amplitude from RMP

Changes in ionic currents secondary to the selective IK_{ur} inhibition in sinus rhythm and atrial fibrillation as revealed by the action potential simulation

The shape and potential domain of the "healthy" right atrial action potential plateau were dependent on the activity of the ICa_L, IK_{ur} and IK_r currents. The intensity of I_{to} reaches its highest value (4.8μA/μF) at 3.1 ms after the onset of the action potential and thereafter decreased quite rapidly. At the time associated with the action potential notch, the intensity of I_{to} was still 0.45 μA/μF. At the climax of the action potential dome (i.e. at 72.5 ms), though, practically no current passed through this type of K^+ channel. The IK_{ur} current becomes activated with kinetics comparable to that of I_{to}, but its inactivation process is absent (or to be more precise it is negligibly slow). Consequently, during most of the repolarization phase,

IK_{ur} acts rather like a simple voltage-dependent current. As the repolarization process proceeds, IK_{ur} becomes gradually deactivated and at voltages below –55 mV the IK_{ur} current no longer flows. In our action potential simulations this voltage limit was reached at APDs longer than 175 ms. Owing to the rapid voltage drop during the fast repolarization phase of the action potential, the evolution of the IK_r activation slackens. In sinus-rhythm, the IK_r intensity reaches its maximum (0.8 μA/μF) at 121 ms, that is by 43 ms after the top of the dome. During the late repolarization of the action potential, IK_r activity gradually diminishes. IK_s gets activated more slowly and at a more positive voltage than IK_r. This more positive activation voltages can not be reached in case of sinus rhythm action potentials. However, the IK_s activity might be positively regulated not only by the membrane voltage but also by $[Ca^{2+}]_i$. Depolarized voltages insufficient for activating IK_s alone and increasing intracellular $[Ca^{2+}]_i$ together do activate IK_s even in normal sinus-rhythm action potentials (provided that IK_s is expressed at a reasonably high density in human atrial myocytes). In our simulations, the maximum IK_s activity was 0.23 μA/μF and reached its peak after 127 ms. Under control conditions, the time course of ICa_L is biphasic with a small transient peak at 10 ms with a slower evolving but greater secondary current ampitude (-3.2 μA/μF) at 68 ms. This biphasic Ca^{2+} entry through ICa_L makes the intracellular Ca^{2+} transient slightly biphasic, as well. The Ca^{2+} transient increases relatively fast and reaches a 23 ms long plateau with a $[Ca^{2+}]_i$ of 1.2 μM. During the action potential dome phase, the Ca^{2+} transient increases further until a maximum of 1.5 μM at 71 ms is reached. $[Ca^{2+}]_i$ then returns to its normal systolic level (0.2 μM). In our action potential model the Ca^{2+} transient persists 150-200 ms longer then the action potential. (**Fig 9A**).

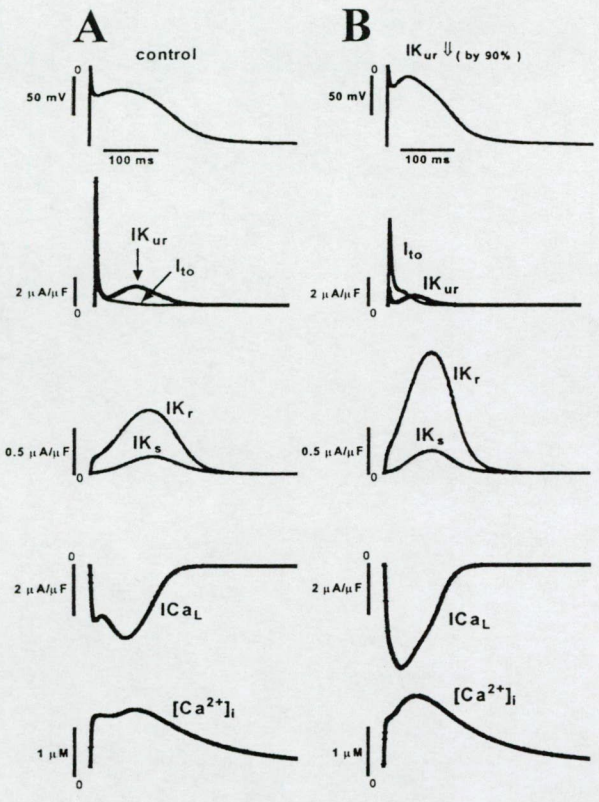

FIGURE 9

The effects of IK_{ur} inhibition on other ionic currents and on the $[Ca^{2+}]_i$ transient in "healthy" human atrial myocytes (computer simulation)

The sarcolemmal Ca^{2+} pump was not incorporated in our model, the removal of the surplus myoplasmic $[Ca^{2+}]$ resides solely in activities of the Na^{+}-Ca^{2+} exchange and the reticular Ca^{2+} pump. Ignoring the very top of the atrial action potential, the exchanger current flows inwardly with a maximum of –4.4 μA/μF at 200 ms. When IK_{ur} is blocked, inward currents through ICa_L and $INaCa_{Ex}$ become unbalanced and notch and plateau potentials get more depolarized. The more positive the plateau and notch potentials are, the more IK_r gets activated and ICa_L and $INaCa_{Ex}$ currrents become couterbalanced again. In this way a 90% inhibition of IK_{ur} causes an 80% increase in IK_r activity. This more intense IK_r repolarizes the membrane more effectively and the resulting APD_{90} value becomes even shorter than it was with unblocked IK_{ur} (in simulation: 220 ms vs. 260 ms as control). An equally significant increase in IK_s activity secondary to a 90% IK_{ur} block was not be seen. Both L-type Ca^{2+} current and the amplitude and time-integral of the Ca^{2+} transient get, however, markedly increased (by 35 and 12 and 13 %, respectively). Owing to the changes in current activities and Ca^{2+} flows, the maximum dome potential is reached earlier too (51 vs. 69 ms as control). (**Fig 9B**, **Fig10**).

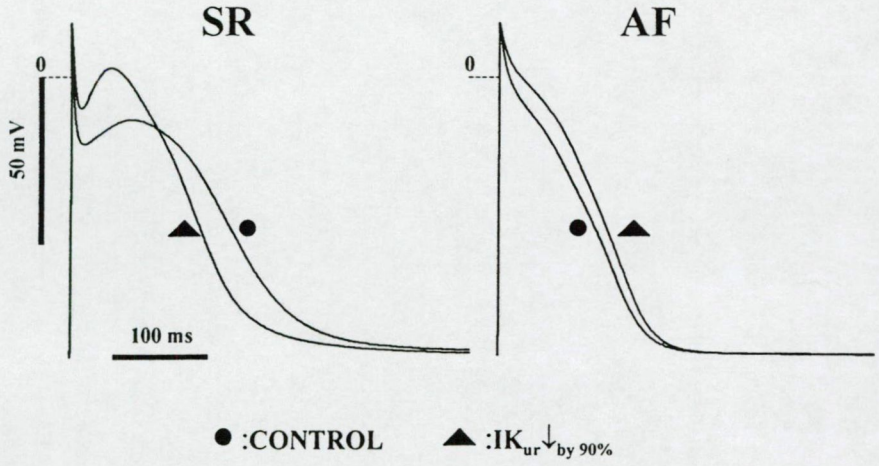

FIGURE 10

The effect of selective inhibition of IK_{ur} on the action potential in sinus-rhythm and atrial fibrillation at a steady-state stimulation of 1Hz (computer simulation)

In the the model for fibrillating atrial myocyte reduced I_{to}, IK_{ur}, IK_s, IK_r and ICa_L currents were incorporated with maximum conductances values of 0.01, 0.003, 0.2, 0.025 and 0.005 mS/μF, respectively (**APPENDIX, TABLE 7**). This resulted in a realistic "fibrillating" action potential form with 21 ms APD_{20}, 155 ms APD_{90} and an average plateau level of -9.5 mV. Here a 90% inhibition of IK_{ur} also brought about a 3% increase in the amplitude of L-type Ca^{2+} current, a 22% enhancement of the $[Ca^{2+}]_i$ transient, and also forced the Na^+-Ca^{2+} exchange to carry more inward current. These effects tended to make the APD longer. The increase in IK_r activity, resulting from the IK_{ur} block–induced depolarization of the action potential plateau from -9.5 to -2.8 mV, was 53%. This augmentation, however, was insufficient to neutralize the increase in intensity of inward currents so a net APD prolongation appeared. When "fibrillating" action potentials with reduced IK_{ur} activity were simulated, APD_{20} and APD_{90} values rose by 98% and 6%, respectively (**Fig 9B**, **Fig 10**).

As the results obtained with our human action potential model revealed, the APD effects of an IK_{ur} block may be strongly modulated by the activity of other delayed rectifiers, especially by the IK_r one.

Modulation of 4-aminopyridine effects by restraining the IK_r activity

In a sinus rhythm preparation, the selective IKr blocker E-4031 though seemed to increase APD_{80} and APD_{90} values, but the changes did not prove to be significant (281.0 ±37.7 ms APD_{80} and 412.1 ±42.8 ms APD_{90} in the presence of 1μM E-4031 vs. APD_{80} and APD_{90} values of 252.2 ±27.5 and 362.3 ±29.5 ms as controls, respectively; n = 5).

TABLE 3
The effect of E-4031 on the 4-aminopyridine–induced action potential changes at a driving rate of 1Hz in human right atrial appendages obtained from patients with sinus-rhythm

	RMP (mV)	AMP (mV)	V_{max} (V/s)	APD_{20} (ms)	APD_{80} (ms)	APD_{90} (ms)	NOTCH (mV)		PLATEAU (mV)		TRIANGULARITY
							abs	**amp**	**abs**	**amp**	
control	-72.4 ±1.1	97.3 ±3.3	280.4 ±30.2	2.1 ±0.5	252.2 ±27.5	362.3 ±29.5	-29.8 ±1.7	42.6 ±2.6	-26.5 ±1.8	45.8 ±2.3	-3.47 ±0.22
+1 μM E-4031	-73.3 ±2.1	96.5 ±3.9	276.5 ±27.1	1.9 ±0.3	281.0 ±37.7	412.1 ±42.8	-30.7 ±1.4	42.6 ±2.7	-28.7 ±1.5	44.7 ±3.1	-3.63 ±0.20
+ 5μM 4-AP	-72.1 ±1.6	90.9 ±6.1	235.5 ±36.7 ★	4.0 ±1.4 §	358.5 ±28.8 ★	483.4 ±32.6 ★	-18.9 ±3.4 §	53.2 ±3.2 §	-14.4 ±2.7 §	57.7 ±2.9 §	-2.83 ±0.78 §

mens±SE, n = 5, §: $p < 0.05$, E-4031 vs. 4-AP; ★: $p < 0.05$, control vs. E-4031+4-AP, **abs**: absolute values, **amp**: amplitude from RMP. Statistical analysis: ANOVA, Dunn's multiple comparison test.

Still, the application of 5μM 4-AP in the presence of E-4031 resulted in significant APD lengthenings both at 80 and 90% repolarization levels, when compared to controls (APD_{80} was increased to 358.5 ±28.8 and APD_{90} to 483.4 ±32.6 ms, [$p < 0.01$]). In the presence of E-4031 alone, there was no significant change on the APD_{20} value. Although having been equilibrated with 1 μM E-4031 for 30 min, E-4031-induced changes in notch or plateau potentials were not observed. However, both of them became more depolarized when 5 μM 4-AP was also applied in the presence of E-4031 (-18.9 ±3.4 and -14.4 ±2.7 mV vs. -30.7 ±1.4 [$p<0.01$] and -28.7 ±1.5 mV [$p<0.05$] notch and plateau potentials for E-4031+4-AP and for E-4031 alone, respectively). In the presence of E-4031 4-AP legthened APD_{20} as well (control: 2.1 ±0.5 vs. E-4031+4-AP: 4.0 ±1.4 ms [$p< 0.05$]) (**TABLE 3, Fig 11**).

The influence of IK_r and IK_s intensities on 4-aminopyridine effects as revealed by the action potential simulation

In action potential simulations, the effects of IK_{ur} blocking on the APD were dependent on the intensities of the IK_r and IK_s currents. A 75% reduction in IK_r conductance resulted in simulated action potentials with an APD_{90} of 313 ms in steady-state. When, in addition, IK_{ur} was reduced by 90% the action potential plateau was elevated from –14.5 to 2.3 mV.

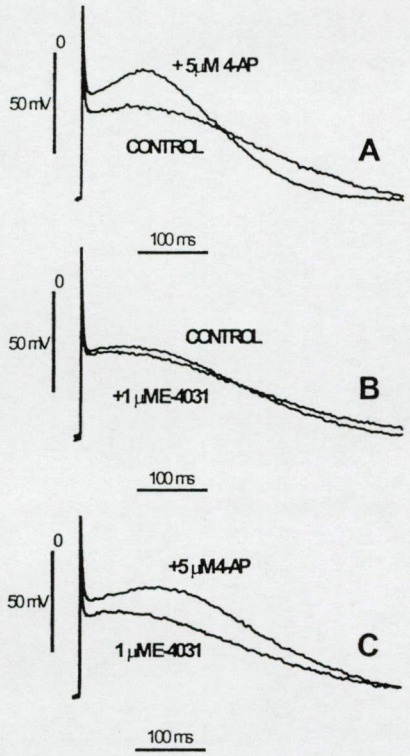

FIGURE 11

The effect of selective IK_{ur} inhibition on the action potential under control conditions (A,B) and after IK_r had been blocked by 1μM E-4031 (C) in "healthy" human right atrial myocardium at a steady-state driving rate of 1Hz

The duration of simulated "sinus-rhythm" action potentials with weak IK_r, however, did not become shorter after reducing the IK_{ur} conductance by 90%. (control APD_{90}: 315 ms vs. APD_{90} with blocked IK_{ur}: 320 ms).

Under control conditions (i.e. with strong IK_r) simulated "sinus-rhythm" action potential forms proved to be insensitive to changes in the IK_s intensity (a 50% reduction in maximum IK_s conductance produced no noticeable change in APD). However, the additional IK_{ur} block always resulted in APD prolongations in simulations with reduced IK_r and IK_s intensities. In such cases a 90% reduction in maximum IK_{ur} conductance lengthened the APD_{90} from 325 to 358 ms.

In the presence of reduced delayed rectifier intensities, the additional IK_{ur} block elevated the voltage and prolonged the duration of the action potential plateau (-15.4 mV and 125 ms with blocked IK_r vs. –3.0 mV and 158 ms with blocked IK_{ur}, and -16.3 mV and 146 ms with blocked IK_s vs. –2.3 mV and 187 ms with blocked IK_s+ IK_{ur}).(**Fig 12**)

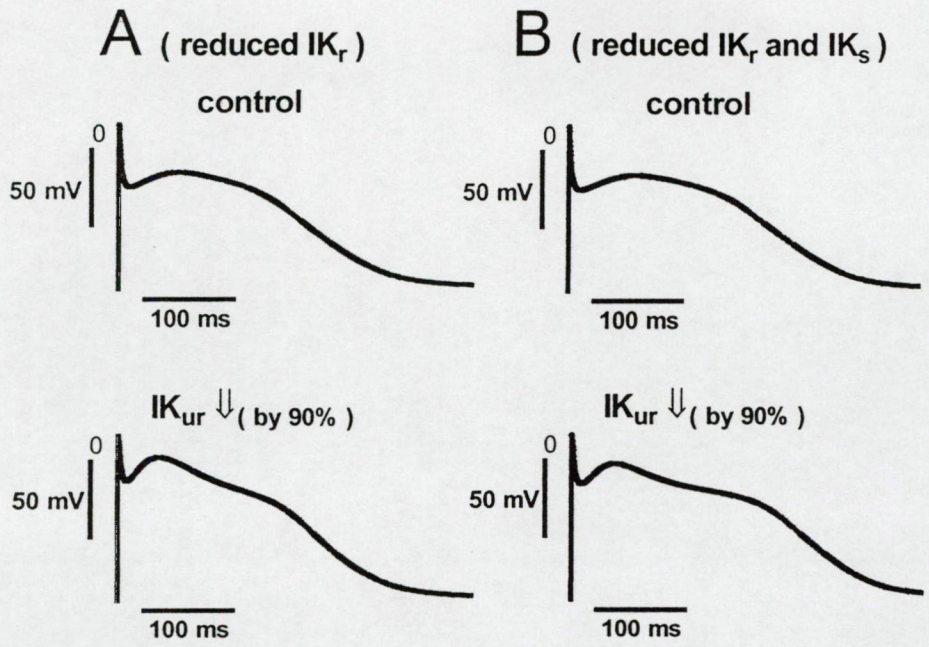

FIGURE 12

In "healthy" atrial myocytes with weak delayed rectifier currents (IK_r and IK_s) 4-AP-induced IK_{ur} block does not shorten the action potential duration (computer simulation)

Effect of IK_{ur} blocking on "sinus-rhythm" action potentials in the presence of carbachol

The pretreatment of sinus rhythm preparations with 1 μM carbachol shortened the action potential duration (175.4 ±10 and 276.7 ±20.8 ms [n=6] vs. untreated 290.8 ±6.3 and 413.6 ±10.4 ms [n=16], APD_{80} and APD_{90}, respectively), shifted the plateau to more negative potentials (-28.4 ±5.8 [n=6] vs. untreated –21.0 ±2.5 mV [n=16]) and slightly hyperpolarized the resting mebrane potential (-75.0 ±1.1 [n=6] vs. untreated -72.4 ±1.1 mV [n=16]). In the presence of carbachol, 4-AP elevated the action potential plateau (from –28.4 ±5.8 to –10.6 ±5.5 mV, [n=6], $p< 0.01$), as was routinelly observed in other preparations too. However, the APD_{80} and APD_{90} were somewhat lengthened (from 175.4 ±10.0 and 267 ±20.8 to 240.4 ±16.1 and 330.8 ±26.8 ms, respectively) by 4-AP after carbachol pretreatment. Other action potential parameters measured in the presence of carbachol remained practically unchanged by an additional 20 min incubation with 4-AP. (**Fig 13**, **TABLE 4**)

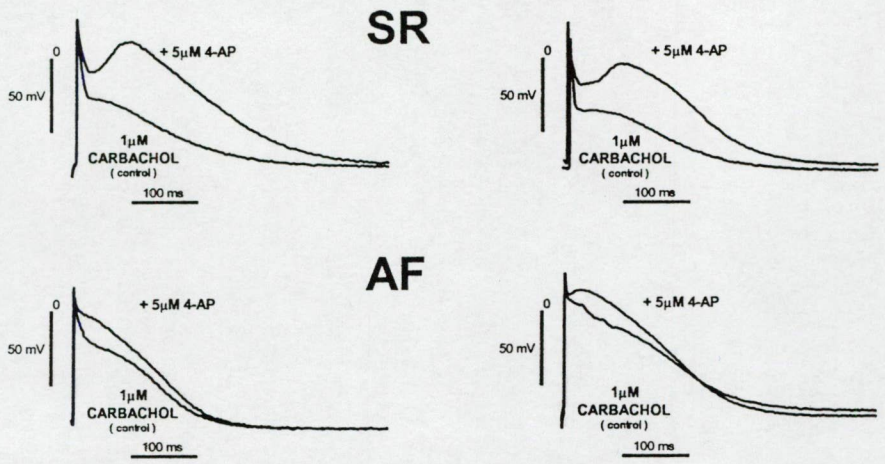

FIGURE 13

Effect of 4-AP on the action potential in sinus-rhythm (SR) and atrial fibrillation (AF) in two representative preparations in the presence of 1 μM carbachol

TABLE 4
Effect of 5-μM 4-aminopyridine
on the action potential parameters in "healthy" human right atrial appendages pretreated with 1 μM carbachol at a driving rate of 1Hz

	RMP (mV)	AMP (mV)	V_{max} (V/s)	APD_{20} (ms)	APD_{80} (ms)	APD_{90} (ms)	NOTCH (mV)		PLATEAU (mV)		TRIANGULARITY
							abs	**amp**	**abs**	**amp**	
control	-75.0 ±1.1	94.2 ±2.1	236.3 ±23.4	7.7 ±4.5	175.4 ±10.0	276.7 ±20.8	-42.8 ±3.6	32.2 ±4.1	-28.4 ±5.8	46.8 ±4.8	-2.36 ±0.43
+ 5μM 4-AP	-73.1 ±1.4	93.6 ±2.1	236.1 ±17.8	20.00 ±11.1 ★	240.4 ±16.1 ★	330.8 ±26.8	-20.6 ±8.9	52.5 ±8.2	-10.60 ±5.6 ★	62.5 ±6.0 ★	-1.97 ±0.65

mens±SE, n = 6, ★: $p < 0.05$, **abs**: absolute values, **amp**: amplitude from RMP

Effect of IK_{ur} blocking on "fibrillating" (AF) action potentials in the presence of carbachol

In atrial trabecular preparations taken from patients with chronic atrial fibrillation the action potential form varied greatly. The treatment of preparations with 1 μM carbachol did not result in any significant APD shortening or in any dramatic change in the chraracteristics of the plateau phase. Exposure of carbachol treated AF trabeculae (n=4) to 4-AP resulted in plateau elevation (from –5.8 ±2.3 to +7.5 ±2.9 mV) without any statistically verifiable change

in APD_{90} values (263 ±15.1 ms as control vs. 272 ±16.7 ms after 20 min incubation with 5 μM carbachol) (**Fig 13**).

Simulation of the effect of IK_{ur} blocking on different ionic currents in the presence of activated IK_{ACh} in "healthy" atrial myocytes

The incorporation of an IK_{ACh} current with 0.07 mS/μF in the atrial action potential model markedly shortens the action potential duration (from 260 to 149 ms at 90% repolarization) shifts the plateau to more negative potentials (from -14.8 to -32.1 mV) and hyperpolarizes the resting potential by 3 mV. The hyperpolarization of the action potential is strong enough to make the Ca^{2+} current weaker during the plateau (maximum current: -2.44 vs. –3.15 μA/μF without IK_{ACh}). The lower depolarizing activity arising from this secondary decrease in the Ca^{2+} current intensity is not capable of keeping back the unbroken evolution of the repolarization and hence neither the notch nor action potential dome can be formed so the restoration of the resting potential can be achieved earlier. Moreover, the faster repolarization without an action potential dome weakens the maximum IK_r and IK_s activities too (from 0.8 to 0.2 and from 0.13 to 0.04 μA/μF, respectively). Under such circumstances, although only small IK_{ur} current flows during the plateau, its role is very important. When IK_{ur} is blocked the speed of the early repolarization slows down. This slower, early repolarization makes ICa_L more intensive, and this secondary activated ICa_L can even reverse the direction of the repolarization for a while, especially after the I_{to} has already been inactivated. The process results in the formation of a characteristic notch. The upward bending dome makes it possible for more IK_r to be activated. And this more intense IK_r then repolarizes the mebrane potential to a level, where the resting potential can be restored by the inward rectifiers alone. With activated IK_{ACh} and unblocked IK_{ur}, the Ca^{2+} influx into the myoplasm decreases, which results in a smaller Ca^{2+} transient, as well. The smaller Ca^{2+} transient brings about a reduction in the rate of the Na^+-Ca^{2+} exchange. The shortening of the APD after IK_{ACh} activation can also be attributed to this accompanying reduction in the exchanger activity. When the IK_{ur} is switched off, the Ca^{2+} transient becomes greater, and the more intensive Ca^{2+} current together with an enhanced inward exchanger current will make APD longer. When a high density of IK_s is supposed and the IK_s is regarded as activated by $[Ca^{2+}]_i$, the elevated myoplasmic Ca^{2+} concentration and the more positive plateau potential resulting from the IK_{ur} inhibition, may theoretically also activate more IK_s. However, even it is so, the Ca^{2+}-induced recruitment of additional IK_s activities remains insufficient in the substitution of the absent IK_{ur} functions for keeping the action potential duration short (**Fig 14,15**).

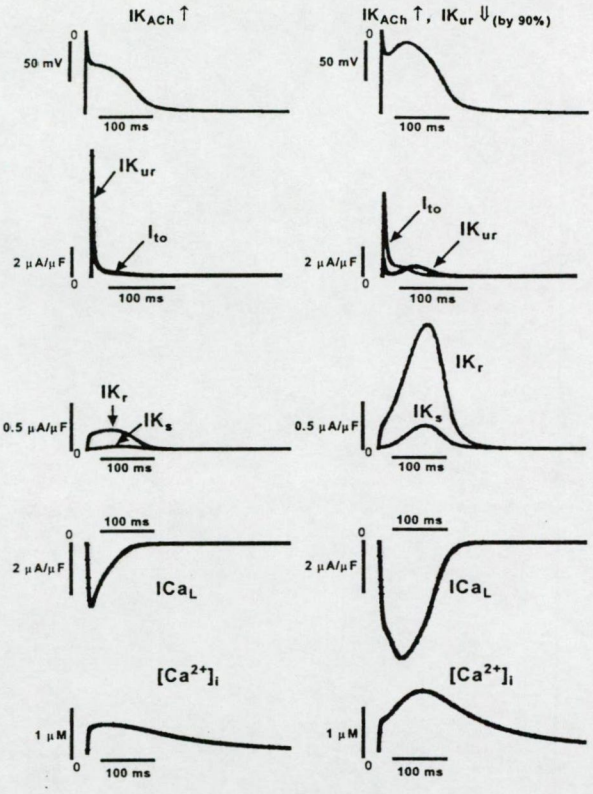

FIGURE 14

Effect of IK_{ur}–inhibition on different current activities and on the time course of the $[Ca^{2+}]$ transient in the presence of activated IK_{ACh} (computer simulation)

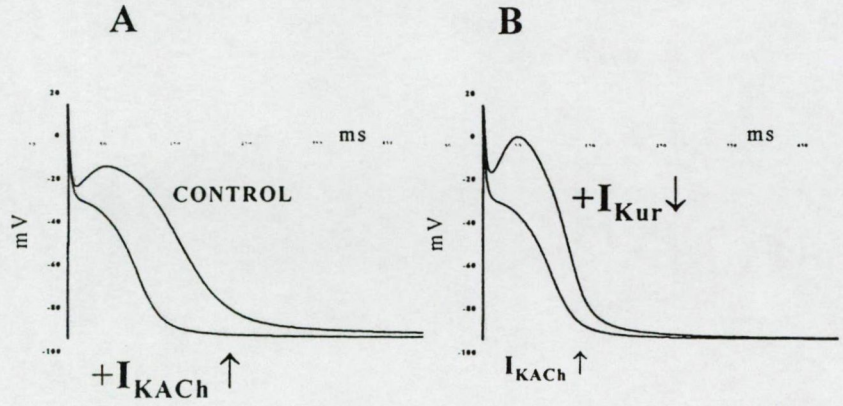

FIGURE 15

In human right atrial action potential models with activated IK_{ACh}, IK_{ur} inhibition lengthens the action potential duration

The effect of 4-aminopyridine on the APD-restitution in the presence and absence of carbachol in sinus rhythm, atrial fibrillation and at 1Hz driving rate

As a tendency, the 4-AP induced restitutional APD changes both in sinus-rhythm and "fibrillating" atrial tissue could be compared with those determined at a 1Hz driving rate. Namely, after 20 min incubation with 4-AP, the APD was shorter practically over the whole diastolic interval (DI) range in sinus-rhythm. However, in "fibrillating" trabeculae or in sinus-rhythm trabeculae pretreated with carbachol, where APD_{80} and APD_{90} values were increased with the application of 4-AP at a 1Hz driving rate, 5 μM of 4-AP induced consequent restitutional APD lengthening. The restitution of the height of the action potential plateau was influenced by 4-AP in a similar way in each groups. Throughout the entire DI range, the plateau occurred at higher membrane potentials in the presence of 5μM 4-AP. **(Fig 16)**

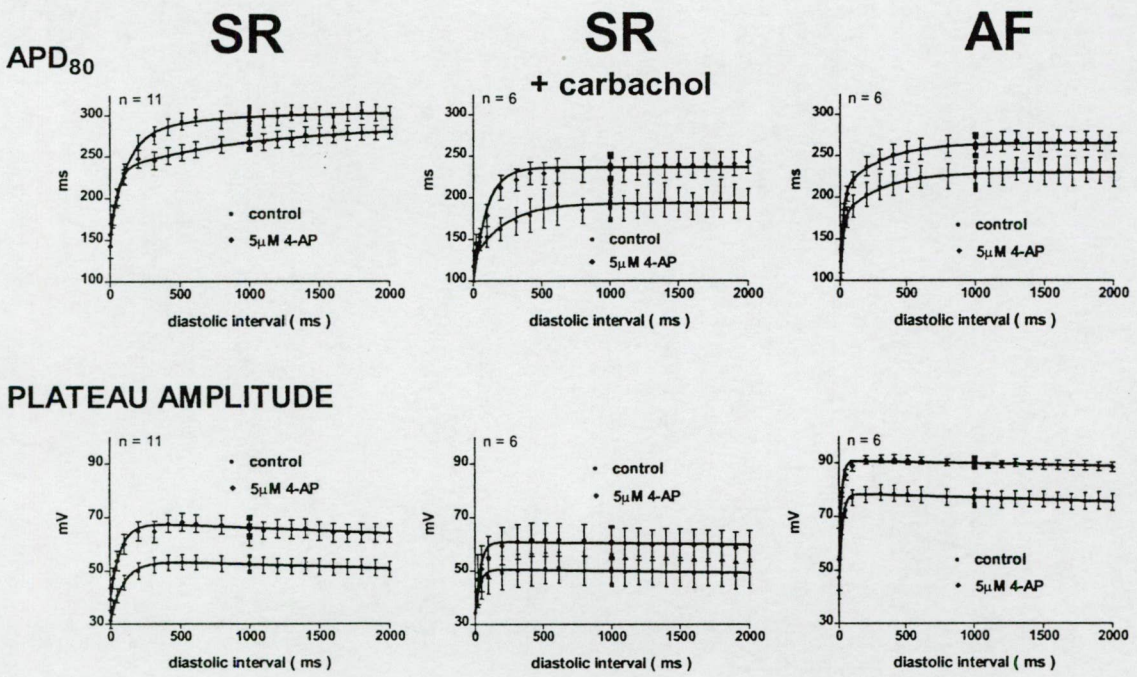

FIGURE 16

The effect of 4-AP on the action potential restitution at a 1Hz basic cycle length in human right atrial trabeculae taken form patients with sinus-rhythm (SR) and chronic atrial fibrillation (AF)

In sinus-rhythm preparations, the plateau restitution markedly followed a biphasic DI-dependence reaching the highest (more depolarized) plateau levels at DIs between 200 and 600 ms. At DIs longer than 1000 ms, the action potential plateau (and also the action potential dome) became gradually smaller (or less expressed). This tedency, though, was

less noticeable in "fibrillating" preparations or in the carbachol pretreated sinus-rhythm group. The highest initial velocity of APD and plateau restitution was measured in "fibrillating" atrial preparations (4.39 ±1.21 ms_{APD}/ms_{DI} and 1.46 ±0.32 $mV_{PLATEAU}/ms_{DI}$, respectively).

TABLE 5
Parameters of the action potential restitution
sinus rhythm (n=11)

parameter	APD		PLATEAU	
	CONTROL	+5 μM 4-AP	CONTROL	+5 μM 4-AP
amplitudes				
A_o	302.7 ± 2.3 ms	278 ± 4.1 ms ★	54.05 ± 0.21 mV	68.20 ± 0.46 mV ★
A_1	119.0 ± 12.7 ms	94.9 ± 3.3 ms	23.03 ± 0.28 mV	29.56 ± 0.67 mV ★
A_2	30.0 ± 11.6 ms	53.4 ± 3.2 ms	0.0016 ± 0.0002 mV/ms	0.0022 ± 0.0004 mV/ms
time constants				
τ_1	110.5 ± 12.1 ms	44.3 ± 3.4 ms ★	96.81 ± 3.34 ms	72.85 ± 4.55 ms ★
τ_2	563.4 ± 243.7 ms	946.8 ± 180.8 ms	ND	ND

sinus rhythm +1 μM carbachol (n=6)

parameter	APD		PLATEAU	
	CONTROL	+5 μM 4AP	CONTROL	+5 μM 4AP
amplitudes				
A_o	193.2 ± 1.0 ms	236.3 ± 1.3 ms ★	50.70 ± 0.31 mV	60.96 ± 0.64 mV ★
A_1	68.4 ± 2.4 ms	140.3 ± 3.1 ms ★	17.57 ± 0.60 mV	34.42 ± 0.98 mV
A_2	ND	ND	0.0007 ± 0.00031 mV/ms	0.0005 ± 0.00056 ★ mV/ms
time constants				
τ_1	223.5 ± 25.0 ms	97.1 ± 7.6 ms ★	33.95 ± 3.1 ms	33.62 ± 2.93 ms
τ_2	ND	ND	ND	ND

atrial fibrillation (n=6)

parameter	APD		PLATEAU	
	CONTROL	+5 μM 4-AP	CONTROL	+5 μM 4-AP
amplitudes				
A_o	229.2 ± 0.6 ms	264.6 ± 0.7 ms ★	78.59 ± 0.27 mV	90.77 ± 0.33 mV ★
A_1	90.1 ± 4.4 ms	118.6 ± 4.9 ms ★	35.26 ± 0.54 mV	43.15 ± 0.71 mV ★
A_2	54.9 ± 3.3 ms	60.1 ± 3.7 ms	0.0015 ± 0.00023 mV/ms	0.0010 ± 0.00028 mV/ms
time constants				
τ_1	20.5 ± 2.6 ms	20.1 ± 2.2 ms	24.03 ± 1.05 ms	18.33 ± 0.91 ms ★
τ_2	291.2 ± 29.3 ms	287.9 ± 29.1 ms	ND	ND

Restitution was modelled by the following equations: APD: $A_o - A_1\exp(-DI/\tau_1) - A_2\exp(-DI/\tau_2)$, PLATEAU: $A_o - A_1\exp(-DI/\tau_1) - A_2DI$, where DI: is the length of the diastolic interval in ms, A_o would be the value of the action potential parameter at infinitely long DI, A_1 and A_2 are maximum amplitudes of the restitutional processes with τ_1 and τ_2 time constants. In case of the PLATEAU restitution the second term was rather linearily dependent on DI with an A_2 slope. Statistical analysis: two sampled Student's t-test, ★:$p < 0.05$; ND: not determined.

The commencement of APD restitution took place at a markedly slower kinetics in sinus-rhythm preparations (1.08 ±0.29 ms_{APD}/ms_{DI}) and it occurred at the slowest rate when sinus rhythm preparations were pretreated with carbachol (0.31 ±0.11 ms_{APD}/ms_{DI}). In all three cases, the initial velocities of both APD and plateau restitutions were uniformly increased by the application of 5 μM of 4-AP. (**Fig 16**, **TABLE 5**).

Other observations on human atrial preparations with 4-aminopyridine

The effects of drugs on frequency dependent or restitutional action potential alterations are frequently analyzed to elucidate antiarrhythmic actions. Since the human atrial preparations under our experimental circumstances proved to be extremely sensitive to any changes in stimulation frequency, the frequency dependent 4-AP effects could not really be investigated in practice. Human atrial trabeculae responded to stimulation protocols rutinely used for cardiac preparations of other types[83,84,85,86] with the shortening of APD, disappearance of the action potential dome and depolarization of the resting mebrane potential. In this respect "sinus-rhythm" preparations tended to perish faster than those from patients with atrial fibrillation. With longer diastolic intervals, the APD in diseased preparations often showed anomalous restitution, and their APD values grew gradually shorter at extrastimulus coupling times over 1000 ms. Although, this could not be proved statistically because of the limited number of preparations, inclination to anomalous restitution seemed to correlate with the severity of the heart insufficiency (i.e. with worsening of the left ventricular ejection fraction). It was also noticed that resposiveness of human atrial preparation to other APD prolonging interventions were sometimes qualitatively different from those of animal preparations, and this difference may even be enhanced by various pathological conditions.

The role of INa in shaping the cardiac action potential as revealed by the application of detajmium in experiments on canine cardiac preparations

The most characteristic action of a large group of antiarrhythmic drugs is the inhibition of INa, which causes a decrease in the conduction velocity. During the action potential plateau phase, the INa window current flows and the intensity of this is an important factor in determining the APD values. The extent of APD changes brought about by the INa block varies among cardiac tissues of different types. It is less prominent in ventricular myocytes and most evident in Purkinje fibers, as was demonstrated with detajmium in canine cardiac preparations. In both ventricular myocardium and Purkinje fibers, 1μM detajmium significantly decreased the action potential amplitude and V_{max}, without influencing the resting and maximum diastolic potentials. In ventricular muscle, the APD value was only slightly affected by the drug. However, in Purkinje fibers 1 μM detajmium induced marked APD shortening[83]. (**Fig 17, ANNEX I**)

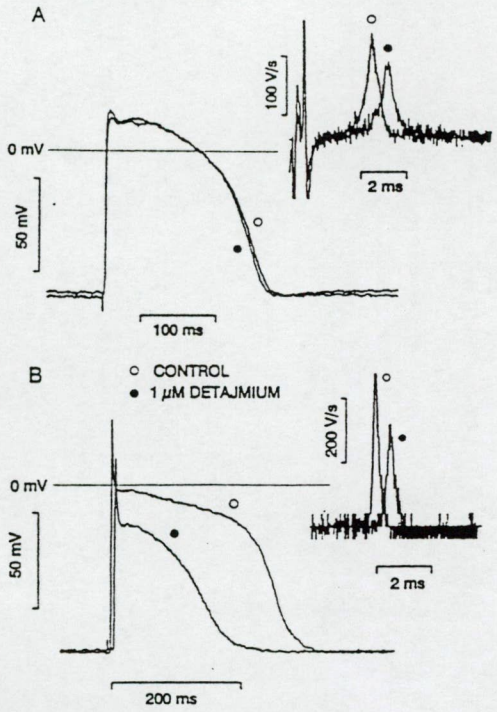

FIGURE 17

The effect of 1μM detajmium on cardiac action potentials in canine ventricular (A) and Purkinje (B) fibers at a cycle length of 1000 ms. Drug-induced changes in the V_{max} are given as inserts on the right side of the figure

Effects of lidocaine on the action potential duration of "healthy" human atrial preparations

The application of lidocain in concentrations below 6 μM did not significantly influence the shape of "healthy" human atrial action potentials at a steady-state driving rate of 1Hz. However, in the presence of 12 μM lidocain, the plateau potential moved to more negative levels (from -12.5 ±3.2 to -21.8 ±2.8 mV) APD_{90} was shortened (from 351.0 ±10.2 to 298 ±5.7 ms) in 3 representative experiments (**Fig 18**).

Effects of tedisamil on human atrial and ventricular action potentials

Tedisamil (1μM) was found to significantly increase APD_{90} in both atrial and ventricular myocardium. The resting potential and action potential amplitude were not altered by the drug. The lengthening of repolarization was more pronounced in the atrial muscle than in ventricular one (28.9 ± 3.3 vs. 13.3±5.2%, n=6, [$p<0.05$]). Furthermore, the drug-induced APD prolongation at 50% repolarization was found to be significant in atrial but not in ventricular preparations. In ventricular myocardium 1μM depressed V_{max} by a small but significant degree. In atrial myocardium, however, the drug effects on V_{max} did not prove to be significant[87]. (**Fig 19**)

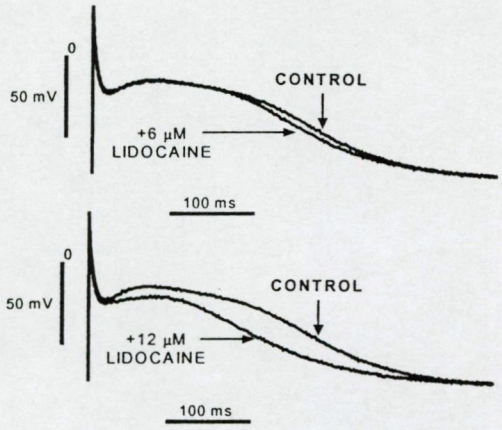

FIGURE 18

Effect of lidocaine on "healthy" human right atrial action potentials at a steady-state driving rate of 1Hz

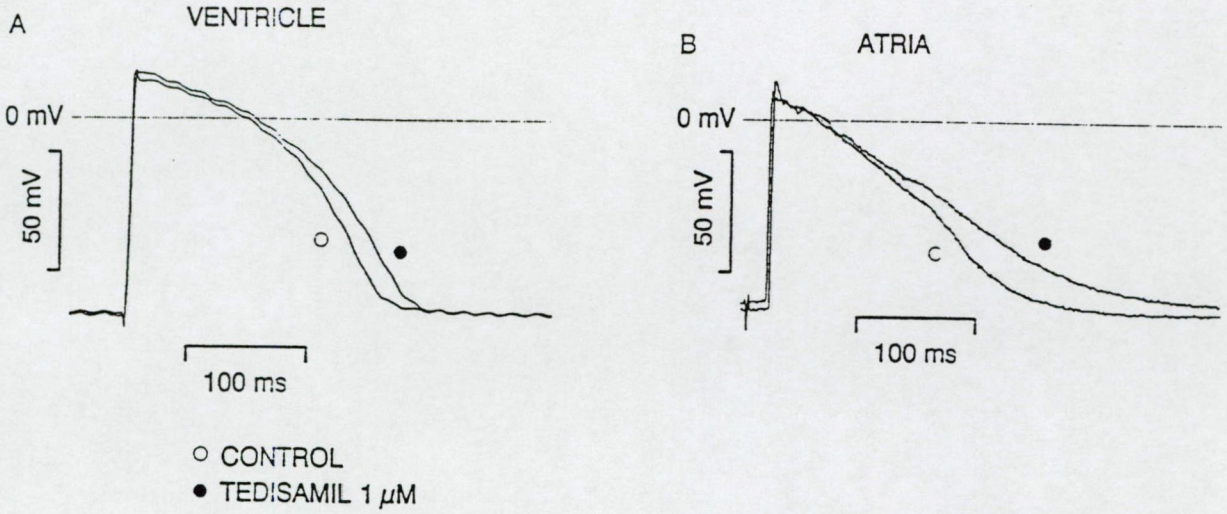

FIGURE 19

Effect of 1 μM tedisamil on the action potential in human ventricular (A) and atrial (B) fiber at a steady-state driving rate of 1Hz

Effects of tedisamil, quinidine and sotalol in rabbit atrial muscle

The effects of these three drugs on repolarization were similar: the APD of action potentials was prolonged by each of them. Out of these drugs, only quinidine reduced V_{max} [85].(**Fig 20, ANNEX II**).

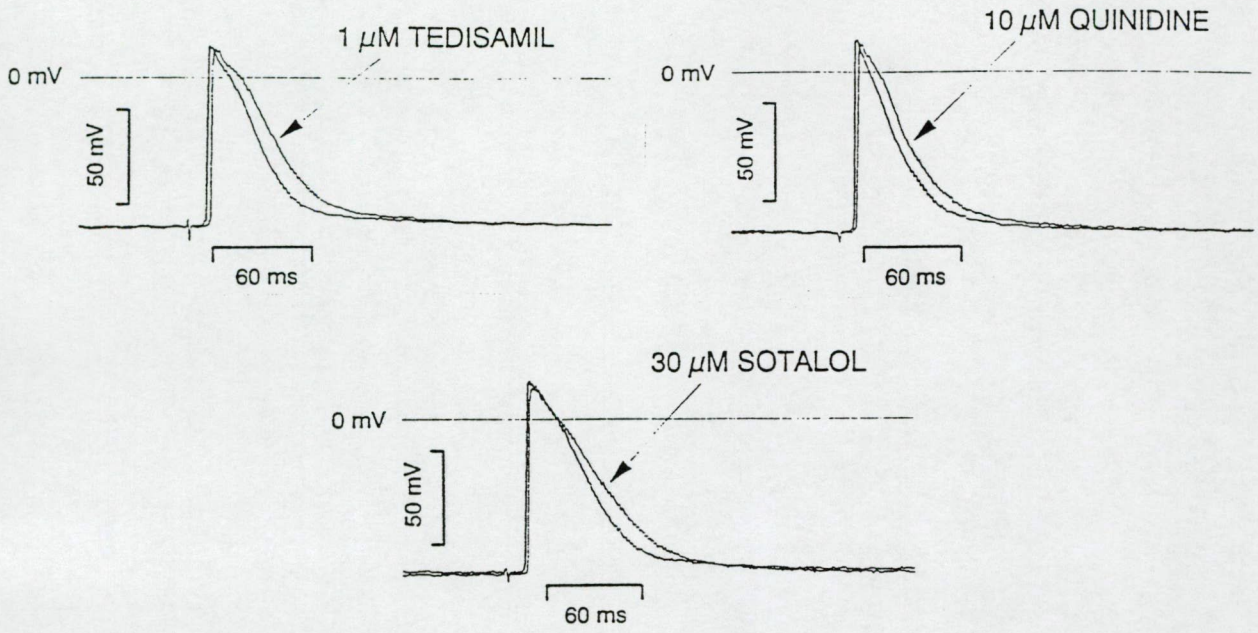

FIGURE 20

Effect of tedisamil, quinidine and sotalol on the action potential in rabbit atrial muscle with a stimulation rate of 1Hz

DISCUSSION

Within human heart, IK_{ur} is exclusively expressed in the atria. According to cardiologists, who argue for the application of channel specific agents as antiarrhythmics, the targeted treatment of atrial tachyarrhythmias could be achieved by selective inhibition of this current. Their view is tacitly based on practical observations with ventricular arrhythmias and also on a common dogma in cardiology. The clinical observations lead them to think, that 1) in ventricular tissue, agents prolonging APD are effective antiarrhythmics at a relatively low risk of proarhyrthmia, and 2) selective agents have side effects that are controllable and less diverse than the nonselective ones. The current dogma is that by blocking a repolarizing K^+ current one will inevitably increase the length of an action potential.

One such example is IK_{ur} which can be selectively blocked using 4-AP. In isolated myocytes EC_{50} values of 30-50 μM were found in patch clamp experiments. With I_{to} (the other 4-AP sensitive current expressed in cardiac tissues) a detectable block can be achieved by applying 4-AP concentrations of 100 μM or above. Our findings here also confirmed the belief that low 4-AP concentrations effectively modify the shape of human atrial action potentials. In isolated tissue preparations, however, the action potential parameters most sensitive to 4-AP were found to be the notch and plateau voltages (with EC_{50} 13-16 μM in right atrial trabeculae from patients with sinus-rhythm). In our experimental circumstances 4-AP – even when applied in concentrations as low as 5μM - could still induce

readily detectable plateau elevations both in "sinus-rhythm" and "fibrillating" trabeculae. The determination of EC_{50} values in trabeculae from subjects with chronic atrial fibrillation could not be carried out, owing to the variability of "fibrillating" action potential forms and the limited number of available preparations. However, 4-AP induced APD changes were found to be different in "sinus rhythm" and "atrial fibrillation". In "atrial fibrillation" with triangular action potential forms, 4-AP clearly lengthened the APD. In "sinus-rhythm" preparations, though, a 4-AP-induced APD shortening was detected.

As the action potential simulations made apparent, the 4-AP-induced APD shortening observed in undiseased (sinus-rhythm) preparations is a result of the close relationship between IK_{ur}, IK_r, IK_s, ICa_L, $INaCa_{Ex}$ and the $[Ca^{2+}]_i$ transient.

The plateau potential of the sinus-rhythm action potentials in our experiments were between -30 and -20 mV under control conditions. If the repolarizing "force" gets reduced because of a selective IK_{ur} block, the depolarizing effect of ICa_L becomes more pronouced and the action potential plateau shifts into a more positive potential range. Plateau potentials above -20 mV, however, activate IK_r more effectively, and the resulting APD will be even shorter than it would have been with unblocked IK_{ur}. The extent of plateau elevation basically depends on the kinetic features of ICa_L and on the existence of a voltage range, where ICa_L does not fully switch off and there is a flow of the ICa_L window current. When the conditions do not favour a proper window current (i.e. the action potential plateau is too short in duration, the plateau voltages are remotely located from the the window domain, action potential notch can not be formed, or too deep notch voltages rapidly ensue), IK_{ur} block-induced APD shortening can not occur.

When IK_r was selectively blocked by E-4031 in sinus-rhythm preparations with low plateau levels, the lengthening of APD turned to be moderate. When 4-AP was applied in the presence of E-4031, the 4-AP induced plateau elevation failed to acivate the IK_r current and consequently the lengthening effect (i.e. K^+ channel block) on APD prevailed. If the IK_s was strong (as was postulated in the action potential model), absent IK_r functions could be substituted to some extent by the activation of IK_s at plateau levels around 0 mV. However, IK_s becomes activated slower than IK_r and the evolution of the maximum IK_s current is delayed. Owing to the kinetics of the process, an enhanced IK_s could keep APDs at their original lengths (i.e. at values before the inhibition of IK_{ur} or the application of 4-AP). This mechanism might be also the reason why in current clamp experiments on isolated "sinus-rhythm" myocytes, APD chages were not found in the presence of low 4-AP concentrations.

In "fibrillating" atrial trabeculae, the action potential plateau was elevated and APD was lengthened by applying 4-AP. But in chronic atrial fibrillation, I_{to} and ICa_L are downregulated. Data on changes in densities of other ionic currents are at present contradictory. It has been shown that the characteristics of intracellular Ca^{2+} handling are

influenced by chronic atrial fibrillation in such a way that the Ca^{2+} sequestering capacity of the sarcoplasmic reticulum becomes reduced. The absence of an I_{to} current decelerates the rate of early action potential repolarization, which – in turn - inhibits the reactivation of ICa_L . Diminution of the ICa_L intensity due to down-regulation, the failure to be reactivated again and also a reduction of $[Ca^{2+}]_i$ transient together result in a decreased $INaCa_{Ex}$ flow in the inward direction. As a result, the APD shortens, the action potential form becomes triangular and mechanical activity disappears. If IK_{ur} is blocked in "fibrillating" atrial myocytes, the elevation of the action potential can not lead to surplus IK_r or IK_s activation and APD lengthens.

The role of M_2 receptor activation in the triggering of atrial rhythm disturbances is nowadays regarded as an established fact. Most effective compounds used in atrial fibrillation also possess IK_{ACh} blocking activity[88]. The activation of M_2 receptors in atrial preparation accelerates the fast repolarization, moves the action potential plateau to more negative voltages, shortens the APD and hyperpolarizes the resting mebrane potential. If K_{ur} is blocked APD prolongation will occur, so long as the secondarily induced plateau elevation remains small and incapable of activating more IK_r.

In subjects with a structural heart disease, the risk a sympathetically triggered or sustained atrial fibrillation is much higher than in other heart patients. At dominance of the sympathetic tone, intracellular level of cAMP is elevated, ICa_L becomes more activated, the intensity of IK_r remains constant or becomes reduced, IK_s is activated and IK_1 may become activated in atrial myocytes. The value of the resting mebrane potential depends on to what extent different cAMP dependent background currents can be counterbalanced by an increase in IK_1. If the mechanisms outlined above hold, the APD of "fibrillating" action potentials of sympathetically mediated types should be prolonged by the inhibition of IK_{ur}.

Cardiac excitation may be viewed as an electrical wave with a wave-front corresponding to the action potential upstroke (phase 0) and a "wave-back" corresponding to repolarization (phase 3). The wavelength is the distance between the wave-front and wave-back and is equivalent to the product of APD and the conduction velocity (CV). Moe and his coworkers[89] demonstrated that simulated cardiac tissue could support multiple reentrant wave-fronts meandering in complex patterns resembling fibrillation, so they proposed the multiple wavelet hypothesis for atrial fibrillation. This hypothesis was later elegantly validated in the experiments of Allessie et al[90]. In cardiac tissue the conduction time (CT) depends also on the wave-front curvature[91]. At a critical curvature, the source of depolarizing currents is too small to bring the resting tissue to its threshold level, and propagation fails (break). When a break occurs along a propagating wavefront a spiral wave takes shape[92,93]. Spiral waves are greatly prone to instability: the core around which the spiral arm rotates is not stationary but meanders through the tissue and they can break up to form multiple waves[94,95], resulting

in appearance of polymorphic tachycardia or even fibrillation in both ventricular[96,97,98] and atrial tissues[90].

In two-dimensional models of cardiac tissue, the models incorporate many automata with resting, excited and refractory states (the bare essentials of a cardiac cell). When sufficient "preexisting" electrophysiological inhomogenities are introduced into the "tissue", cardiac waves spontaneously break up into random reentry[99]. In Moe's simple model this was achieved by randomly introducing local differences in the APD to cells throughout the tissue. In Moe's model, the heterogeneity was static, and was maintained throughuout the whole simulation procedure. Dynamic heterogeneity is another mechanism that requires a preexisting heterogeneity of some kind to create the first wavebreak. After that, the wavebreak proceeds spontaneously on its own. This type of wavebreak is primarily determined by the electrical restitutional properties, i.e. the dependence of APD and CV values on the preceeding DI, defined as the interval between repolarization and the next action potential. The APD and CV values are therefore key determinants of the wavebreak process. The steepness of APD restitution is also a critical parameter for spiral wave stability. When the slope of APD restitution exceeds a certain value, a small change in DI is amplified into a large change in APD. This in turn creates a larger change in DI for the next wave, and so on. The positive feedback causes small wavelength oscillations to progressively grow until DI becomes too short for the wave to propagate, resulting in a wavebreak. In contrast, a flat APD restitution acts like an attenuator, allowing perturbations in the wave to heal rather than expand[100]. By reducing APD restitution steepness, spiral wave breakup can be prevented and spiral wave behavior can be progressively stabilized. This concept is termed as the restitution hypothesis[101] and has now been validated in several experimental models[102,103]. A natural consequence of steep APD restitution is the APD alternants. When they occur in the ventriculi they are electrophysiologically manifested as T-wave alternants (a clinically established harbinger of arrhythmia vulnerability[104]). This alarming connection between the steepness of the restitution and the propensity for the occurrence of APD alternants can readily be seen when the restitution is measured with stimulation protocols which alternately vary DI as was done in studies undertaken here.

The action potential restitution was altered by 4-AP both in "sinus-rhythm" and "fibrillating" atrial trabeculae in a similar manner as to the way in which the action potential characteristics were altered by the drug at a steady-state stimulation rate of 1Hz. When compared to the control, the height of the plateau amplitude was found to be higher and the APD was shorter throughout the whole DI range (in the presence of 4-AP) in "sinus rhythm" preparations. In trabeculae taken from patients with chronic atrial fibrillation, where the drug-induced plateau elevation was accompanied by APD lengthenings at 1Hz, APD restitution was also delayed by the application of 4-AP (i.e. restitutional APD was always longer in the

presence of 4-AP than under control conditions). Shortened restitutional APDs after M_2 receptor activation were subsequently lengthened by applying 4-AP at all DIs. Compared with "sinus rhythm" preparations, the initial steepness of APD restitution was always higher in "fibrillating" trabeculae. The enhanced initial steepness of APD restitution was also observed with monophasic action potential measurements in patients and is regarded as a malign factor in the generation of atrial fibrillation[105]. Irrespective of the type of preparation (i.e. sinus-rhythm or "fibrillating"), the initial steepness of APD restitution was always enhanced by adding 4-AP in our experiments. Taking into account this latter observation and the 4-AP-induced changes in APD restitution, 4-AP might exert antiarrhythmic actions in atrial fibrillation and in stages with predominance of the parasympathetic tone, but its effects on the electrical activity of the "healthy" atrial myocardium should rather be regarded as proarrhythmic. The potential proarrhythmic feature of 4-AP is also supported by the observation that action potential forms both in "sinus-rhythm" and "atrial-fibrillation" preparations were brought into a more triangular configuration. In ventricular tissue with diverse cellular elements, drugs generating more triangular action potential forms also possess enhanced proarrhythmic capabilities[10].

The secondary effects of the 4-AP -induced IK_{ur} block on the intensity of iCa_L and the $[Ca^{2+}]_i$ transient may also be hazardous to patients in atrial fibrillation or in the prefibrillatory stages with an electrical remodelling in progress. It is generally accepted today that the disruption of $[Ca^{2+}]_i$ homeostasis plays a crucial role in the initiation of electrical remodelling and thereby in the perpetuation of atrial fibrillation[36,46].

Ca^{2+} enters the atrial cells through voltage-, receptor- and "source"-operated channels. Then the Na^+-Ca^{2+} exchanger and less importantly a sarcolemmal Ca^{2+} pump are responsible for its removal. The inward-flowing Ca^{2+} ions (Ca^{2+}-induced Ca^{2+} release) and also the rapid depolarization in during the onset of the action potential (voltage-induced Ca^{2+} release) mobilize Ca^{2+} from intracellular stores. In ventricular cells the Ca^{2+}-induced Ca^{2+} release is brought about by an interplay between the L-type Ca^{2+} channels and the ryanodine-receptors in the T-tubules. In atrial cells the T-tubular system is less developed and a significant portion of the sarcoplasmatic reticulum is not attached to the sarcolemma (corbular sarcoplasmic reticulum). This also means, that in atrial myocardium ryanodin receptors may operate independently of the L-type Ca^{2+} channels. The corbular sarcoplasmic reticulum contains other Ca^{2+} releasing receptors regulated by intracellular second messengers (i.e. inositol triphosphates, diacylglycerol, or nicotine-andenosine-nucleotides). Ca^{2+} ions released into the myoplasm are taken up by the sarcoplasmic reticulum via the reticular Ca^{2+} pump and by the mitochondria. In the sarcoplasmic reticulum Ca^{2+} is sequestered and stored by Ca^{2+} binding proteins. Previously these Ca^{2+} binding proteins were thought to play only a passive role. Today it seems that reticular Ca^{2+} binding proteins

possess a signalling role in gene transcriptions and in events leading to apoptosis. The primary role of Ca^{2+} entering the mitochondria is to regulate the rate of ATP production with ATP requirements of ion-pumps and mechanical activity. Excess Ca^{2+} in the mitochondria also leads to a release of apoptotic mediators into the myoplasm[106]. (**Fig 21**)

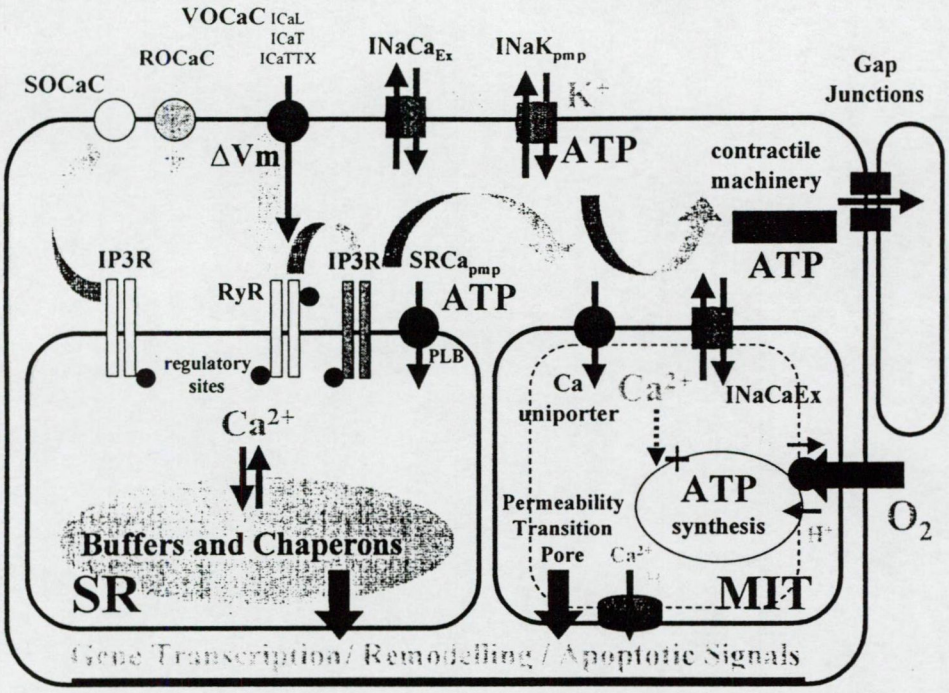

FIGURE 21

Connection between intracellular Ca^{2+} homeostasis and remodelling and apoptosis in chronic atrial fibrillation

The connection between changes in $[Ca^{2+}]_i$ and the cell-cycle is well documented in the literature. In some cases $[Ca^{2+}]_i$ elevations leading to cell proliferation are introduced by the upregulation of K^+ channels. In neurons, the normal expression pattern of ion-channel genes requires rhythmically fluctuating low level intracellular Ca^{2+} concentrations. The increased stimulus frequency in atrial flutter and fibrillation[39] means, for the cell, an increased burden of the Ca^{2+} load. Depending on the activation sequence of various Ca^{2+} signalling systems, both in the myoplasm and in the cell-organelles, response patterns ranging from altered protein expression to myocardial hybernation and apoptosis may emerge (**Fig 22**). It follows - from the central role of $[Ca^{2+}]_i$ in the pathomechanism of atrial fibrillation - that antiarrhythmic drugs become less suitable for the treatment of atrial flutter or atrial fibrillation the more they elevate secondarily the intracellular Ca^{2+} concentration. It is worth noting, that for repolarization lengthening (Class 3) drugs in ventricular arrhythmias, it was always positive argued that they did not reduce the contractile force or even were able to increase the inortopy. However, the atrial tissue is more sensitive than the ventricular and any

increase in the "fibrillating" $[Ca^{2+}]_i$ tends to promote aggravation of the disease. This may also provide an explanation for the increasing ineffectiveness of antiarrhyrthmics over time in the treatment of chronic atrial fibrillation. It is worth mentioning that cardiac glycosides tend to worsen reverse remodelling[107] while verapamil delays the structural remodelling of atrial myocytes in animal models[108].

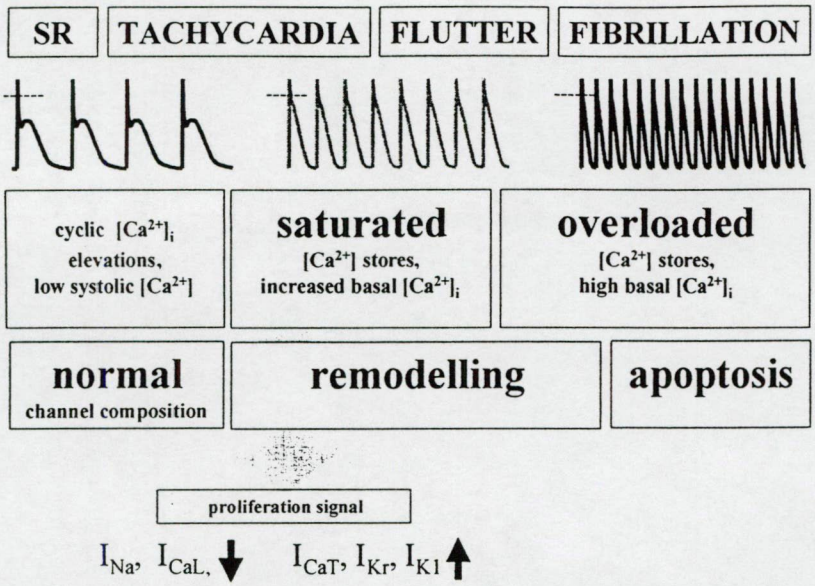

FIGURE 22

The dependence of ion channel remodelling and apoptosis on electrical activity and the extent of the Ca^{2+}-load in atrial myocytes

As computer simulation revealed, the effects of 4-AP on IK_{ur} are inevitably followed by an increase in the $[Ca^{2+}]_i$ transient. But this means that even though IK_{ur} blocking had some antifibrillatory benefits in chronic atrial fibrillation (APD was prolonged and action potential restitution was delayed by 4-AP in trabeculae taken from subjects with chronic atrial fibrillation), the accompanying increase in $[Ca^{2+}]_i$ has a tendency to prevent the complete recovery of the diseased (remodelled) fibrillatory state.

Our results also highlight the rule that what is true for the ventriculi (i.e. if a channel/current has a repolarizing function, an antiarrhythmic effect should be achieved via its inhibition) is not necessarily true for atrial tissues. As it has also been demonstrated in most of our atrial action potential simulations, in atrial myocytes the interplay between ionic currents and changes in the ionic composition of the intracellular millieau is very complex and pharmacological interventions may result in effects that a reductionistic cardiophysiological logic fails to predict or imagine beforehand.

Computer simulation is an important tool for investigating possible causal connections between channel and transporter functions in cardiac myocytes. In our study, the importance of IK_r and IK_s currents in the modulation of 4-AP-induced APD changes was revealed by action potential simulations. As was also experimentally demonstrated application of an IK_{ur} blocker with an IK_r blocker in combination, can minimize the proarrhythmic action potential effects of the IK_{ur} block. With such a combination the IK_{ur}-block-induced APD shortening could effectively be halted or even a net APD lengthening could be achieved. On the other hand, in the therapeutical application of an IK_{ur}+iK_r blocker combination, doses of the IK_r blocker could also be reduced, which would also reduce the risk of unwanted side effects, first and foremost arrhythmias of the "torsade" type.

LIMITATIONS OF THE MODEL

Action potential models are frequently used in electrophysiology. The application of models is inevitable for the integrative interpretation of experimental results obtained under the extremely aphysiological circumstances of the patch-clamp technique. In the more physiological multicellular preparations (due to the unrestricted physiological interplay between the elementary functions) actions seen in patch-clamp experiments can not always be verified persuasively. A scientific interpretation of such discrepancies is practically impossible without using computer models. However, the accuracy of the models is basically dependent on the accuracy of the experimental data. In the present action potential model, published maximum conductance values for ionic currents were used. Some of these conductances had to be readjusted in order to get typical multicellular action potential forms for a steady-state stimulation rate of 1Hz. (**APPENDIX, TABLE 7**). The gating equations for INa and ICa_L had to be re-formulated (**APPENDIX, TABLE 8**) because the relevant formalism available in the literature at present cannot be regarded as sensible either from a physiological or a computational point of view. Our equations yielded exactly the same voltage dependencies for steady-state and time constant values of the relevant gating variables as if they had been calculated using the traditional mathematical expressions.

In this respect it is worth noting, that most action potential models treat the channel gating as if it could be represented by some set of simple open-closed state transitions. The whole channel gating is of course, a rather more complicated process. Fifty years of voltage clamp studies on ionic channels have yielded a wealth of kinetic data and the need to interpret this enormous set of data has led to empirical models in which gating consists of charge translocation between a finite (but large) number of discrete, so-called Markovian[109] states[110,111,112]. This discrete-state Markov models operating with forward and backward rate constants on the analogy of chemical reactions[113] have been very successful in reproducing

the time course of native channel currents, but they lack a physical interpretaion that is consistent with properties of large channel proteins[114]. If it is so, and our present views on elementary channel processes are only fictions, the application of the traditional formalism cannot be regarded as an imperative.

In our model the same compartments for ion-movements were taken into account as those in the Luo-Rudy (LR) model[78] (**APPENDIX, Fig 23**). However, the LR-model was specifically intended for guinea pig ventricular cells. Readjusting of compartment sizes to suit the situation in human atrial tissue was prevented by a scarcity of relevant data.

The compartment sizes and the kinetics of the ion movements through and between the different compartments (especially for Ca^{2+}), however, may directly influence sarcolemmal channel functions. Without an accurate representation of the simulated intracellular Ca^{2+} movements, a realistic human atrial action potential model can not be imagined.

In our model, the intracellular Ca^{2+} handling was modelled in the same way as that by Zeng et al[77]. Although Ca^{2+} handling of this type proved to be a good choice in our model, it cannot be regarded as to be perfect. It does not take into consideration reticular Ca^{2+}-release channels except ryanodine receptors and does not include reticular Ca^{2+} buffers beyond calsequestrin. Even this Ca^{2+} handling model regards the ryanodine receptors as passive Ca^{2+} -regulated pores without any rectification. None of the models having been published so far, took Na^+, K^+ and Cl^- channels in the subcellular membranes into consideration. Effects of drugs on ionic channels in membranes of cell organelles may also influence Ca^{2+} movements and thereby Ca^{2+}-regulated sarcolemmal ionic channels too. Action potential models ignore mitochondria, though their role in the Ca^{2+} homeostasis is well known.

In our model, direct regulation by $[Ca^{2+}]_i$ was postulated only for ICa_L, IK_s and IK_{Ca}. However, INa and most of the K^+ currents are also known to be influenced by intra or extra-cellular Ca^{2+} ions.

Effects mediated by intracellular second messengers such as cAMP, cGMP, muscarinergic effects but the activation of IK_{ACh} were not taken into account here.

The role of IK_r in resting myocytes has probably been overestimated. Under experimental circumstances the blocking of this current did not cause APD to such an extent that was predicted by the model. The maximum conductance of IK_s in the model is about 10 times greater than the relevant values found in myocardial preparations. The rectifying properties of K^+ channels was regarded as merely a voltage dependent process, and a block by divalent cations or intracellular polyamines was not incorporated into the model.

Performace of the model was not tested in simulations for APD restitution or frequency-dependence. Our goal here was to test and simulate effects at 1Hz.

SUMMARY

Therapeutical Implications

We have seen that by inhibition of the atrial specific IK_{ur} current, antiarrhythmic/antifibrillatory effects can be expected in "fibrillating" atrial myocytes and in "healthy" atrial tissue with overwhelming parasympathetic dominance. For a long-term therapeutical application, due to the secondarily induced changes in the $[Ca^{2+}]_i$ homeostasis, the effectiveness of IK_{ur} blockers however seems to be uncertain.

Antiarrhythmic potency of IK_{ur} blockers may be enhanced by combination with IK_r blockers. In "healthy" human atrial myocytes IK_{ur} blockers alter action potential parameters and also the action potential restitution with a rather proarrhythmic profile. Application of IK_r blockers (dofetilide or sotalol) in combinations with IK_{ur} blockers could reduce the possible enhancement of the risk to develop or to favour atrial fibrillation due to the shortening of the action potential duration and effective refractory period caused by the IK_{ur} block in sinus rhythm. A possible advantage of combining IK_{ur} and IK_r block over IK_{ur} block alone, seems to be that doses of IK_r blockers could be reduced.

Importance of action potential simulations

Our results also highlight that the rule what is true for the ventriculi (i.e. if some channel/current has a repolarizing function, via its inhibition an antiarrhythmic effect should be achieved) is not necessarily true for atrial tissues. As it has also been proved by our atrial action potential simulations, in atrial myocytes the interplay between ionic currents and changes in ionic composition of the intracellular millieau is very complex and pharmacological interventions may result in effects unforeseen to a reductionistic cardiophysiological logic.

Computer simulation is an important tool in discovering potentially existing relationships between channel and transporter functions in cardiac myocytes. In the present study, importance of IK_r and IK_s currents in modulation of 4-AP-induced APD alterations was revealed by action potential simulations at first.

APPENDIX

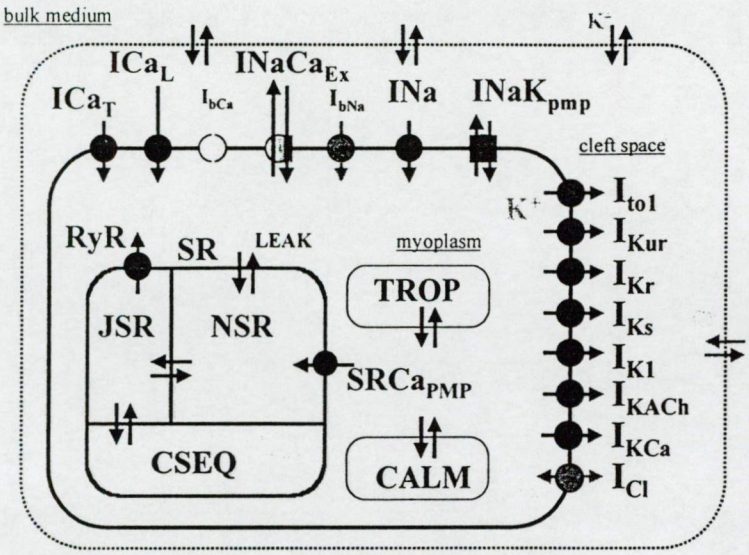

FIGURE 23

Schematic representation of currents, pumps and exchangers included in the model
The model consists of 5 compartments: the bulk medium, cleft space, myoplasm and junctional and network sarcoplasmic reticulum (JSR and NSR).

TABLE 6

ABBREVIATIONS EMPLOYED IN THE MODEL

in alphabetical order

α or β: forward or backward rate constants in the model, otherwise pore forming or regulatory channel subunits
Δ: change in the indexed parameter between two integration steps
γ: relative mebrane distance (see equations for $INaCa_{Ex}$)
τ: time constants
Δt: length of the integration step
a: probability of channel activation (except INa)
b: probability of channel inactivation (except INa)
bCa: Ca^{2+} dependent inactivation
CALM: calmoduline
CICR: Ca^{2+}-induced Ca^{2+} release
CSEQ: calsequestrine
E: Nernst's potential
f: function of the indexed variable
$\mathbf{f_{scale}}$: scaling factor (see $INaCa_{Ex}$)
g: conductance
$\mathbf{I_{bCa}}$, or $\mathbf{I_{Bkg,Ca}}$: background Ca^{2+} current
$\mathbf{I_{bNa}}$, or $\mathbf{I_{Bkg,Na}}$: background Na^+ current
$\mathbf{ICa_L}$: L-type Ca^{2+} current
$\mathbf{ICa_T}$: T-type Ca^{2+} current
$\mathbf{I_{Cl}}$: background Cl^- current
$\mathbf{I_f}$: pacemaker current (not included in our model)
$\mathbf{IK_1}$: inward rectifier K^+ current
$\mathbf{IK_{ACh}}$: acetylcholine activated K^+ current
$\mathbf{IK_{Ca}}$: Ca^{2+} activated K^+ current
$\mathbf{IK_r}$: rapid component of the delayed rectifier K^+ current

IK_s: slow component of the delayed rectifier K^+ current
IK_{ur}: ultrarapid delayed rectifier K^+ current
INa: fast Na^+ current
$INaCa_{Ex}$: Na^+-Ca^{2+} exchanger current
$INaK_{pmp}$: Na^+-K^+ pump current
I_p: non selective plateau current (not included in model)
I_{to} or **I_{to1}**: transient outward K^+ current
I_{to2}: Ca^{2+} activated Cl^- current (not included in model)
J: ion fluxes
JSR: junctional SR
Kd: dissociation constants
kQ10: temperature coefficient
k_{sat}: saturation constant (see $INaCa_{Ex}$)
leak: Ca^{2+} leak from the network SR
NSR: network SR
on, off: synonyms for activation (on) and inactivation (off)
over: overload
RyR: ryanodine receptor
SR: sarcoplasmic reticulum
$SRCa_{pmp}$: SR Ca^+ pump
ss (in index): steady-state
Thr: threshold
trans: simple ion transport via diffusion
TROP: troponine
Up: uptake
V_m: membrane potential
VOL: volume
VOLR: volume ratio of the indexed compartments
X: ion in general
z: valence of an indexed ion

TABLE 7

CONSTANTS AND INITIAL PARAMETER VALUES

Parameter	Value
R: gas constant	8.314 J/K/mol
T: temperature	310 K
F: Faraday constant	964867 C/mmol
C_m: membrane capacitance	1.000 $\mu F/cm^2$
A_{Cap}: capacitive mebrane area	1.53E-04 cm^2
VOL_{cell}: cell volume	3.80E-08 ml
VOL_{myo}: volume of the myoplasm	2.47E-08 ml
VOL_{SR} volume of the sarcoplasmic reticulum (SR)	3.80E-09 ml
VOL_{NSR}: volume of the network SR	2.47E-09 ml
VOL_{JSR}: volume of the junctional SR	1.33E-09 ml
VOL_{cleft}: volume of the intercellular space	4.94E-09 ml
ionic concentrations in the bulk medium	
$[K^+]$	4.50E+00 mM
$[Na^+]$	1.44E+02 mM
$[Ca^{2+}]$	1.31E+00 mM
$[Cl^-]$	1.14E+02 mM
ionic concentrations in the cleft space	
$[K^+]_{cleft}$ or $[K^+]_o$	4.50E+00 mM
$[Na^+]_{cleft}$ or $[Na^+]_o$	1.44E+02 mM
$[Ca^{2+}]_{cleft}$ or $[Ca^{2+}]_o$	1.31E+00 mM

$[Cl^-]_{cleft}$ or $[Cl^-]_o$	1.14E+02 mM
ionic concentrations in the myoplasm	
$[K^+]_i$, $[K^+]_{cell}$ or $[K^+]_{myo}$	1.60E+02 mM
$[Na^+]_i$, $[Na^+]_{cell}$ or $[Na^+]_{myo}$	7.02E+00 mM
$[Ca^{2+}]_i$, $[Ca^{2+}]_{cell}$ or $[Ca^{2+}]_{myo}$	2.88E-04 mM
$[Cl^-]_i$, $[Cl^-]_{cell}$ or $[Cl^-]_{myo}$	6.90E+00 mM
parameters for Ca^{2+} handling by the SR	
NSR $[Ca^{2+}]$ (at rest)	8.12E-02 mM
NSR $[Ca^{2+}]_{max}$ (maximum Ca^{2+} concentration in NSR)	3.00E+00 mM
NSR Ca^{2+} uptake Kd (ie. SERCa or $SRCa_{pmp}$)	9.00E-03 mM
NSR Ca^{2+} uptake maximum rate	1.00E-02 mM/ms
NSR Ca^{2+} transfer to JSR (τ)	1.80E+01 ms
NSR Ca^{2+} uptake rate (at rest)	3.11E-04 mM/ms
NSR Ca^{2+} leak rate (at rest)	2.71E-04 mM/ms
NSR Ca^{2+} transfer rate (at rest)	7.76E-05 mM/ms
JSR $[Ca^{2+}]$ (at rest)	7.99E-02 mM
JSR Ca^{2+} overload rate constant (τ)	2.00E+01 1/ms
JSR Ca^{2+} time constant for CICR „on" in overload	4.00E+00 ms
JSR Ca^{2+} time constant for CICR „off" in overload	3.00E+00 ms
JSR Ca^{2+} overload induced release (at rest)	1.49E-29 mM/ms
JSR threshold of voltage induced Ca release	-2.00E+01 mV
JSR CICR rate konstant	1.00E+01 1/ms
JSR CICR rate (at rest)	7.06E-06 mM/ms
TROPONIN $[Ca^{2+}]$ (at rest)	8.85E-04 mM
TROPONIN $[Ca^{2+}]_{max}$	7.00E-03 mM
TROPONIN Ca^{2+} Kd	2.00E-03 mM
CALMODULIN $[Ca^{2+}]$ (at rest)	5.42E-03 mM
CALMODULIN $[Ca^{2+}]_{max}$	5.00E-02 mM
CALMODULIN $[Ca^{2+}]$ Kd	2.38E-03 mM
CALSEQUESTRIN $[Ca^{2+}]$ (at rest)	2.33E-01 mM
CALSEQUESTRIN $[Ca^{2+}]_{max}$	9.00E+00 mM
CALSEQUESTRIN Ca^{2+} Kd	3.00E+00 mM.
CALSEQUESTRIN Ca^{2+} overload threshold	8.75E+00 mM
INa	
g_{max}	1.50E+01 mS/µF
m_{GATE} (at rest)	5.17E-04
h_{GATE} (at rest)	9.97E-01
j_{GATE} (at rest)	1.00E+00
ICa_T	
g_{max}	5.00E-02 mS/µF
a_{GATE} (at rest)	5.04E-02
b_{GATE} (at rest)	8.29E-01
ICa_L	
g_{max}	1.00E-01 (SR) mS/µF or 5.0E-03 (AF)
a_{GATE} (at rest)	4.48E-06
b_{GATE} (at rest)	9.40E-01
Ca^{2+}-iduced inactivation, Kd	4.00E-04 mM
I_{to}	
g_{max}	1.60E-01 (SR) mS/µF or 1.0E-02 (AF)
a_{GATE} (at rest)	1.67E-02
b_{GATE} (at rest)	1.00E+00
IK_{ur}	
g_{max}	3.00E-02 (SR) mS/µF or 3.0E-03 (AF)
a_{GATE} (at rest)	1.97E-04

b_{GATE} (at rest)	9.91E-01
IK_r	
g_{max}	5.00E-02 (SR) mS/μF or 5.0E-03 (AF)
a_{GATE} (at rest)	2.00E-04
Kd for $[K^+]_{o(CLEFT)}$	5.40E+00 mM
IK_s	
g_{max}	6.00E-01 (SR) mS/μF or 2.0E-01 (AF)
Kd for $[Ca^{2+}]_i$	5.00E-04 mM
a_{GATE} (at rest)	2.13E-02
IK_1	
iK1 g_{max}	6.00E-02 mS/μF
IK_{ACh}	
g_{max}	7.00E-04 mS/μF or 7.00E-02
K^+ permeability	8.00E-07 cm/s
Kd for $[Ca^{2+}]_{i(MYOPLASM)}$	4.00E-03 mM
IK_{Ca}	
g_{max}	8.00E-07 cm/s.
Kd for $[Ca^{2+}]_i$	4.00E-03 mM
$I_{Bkg,Na}$	
g_{max}	1.00E-04 mS/μF
$I_{Bkg,Ca}$	
g_{max}	1.00E-06 mS/μF
$I_{Bkg,Cl}$	
g_{max}	9.00E-03 mS/μF
$INaCa_{Ex}$	
I_{max}	1.50E+00 μA/μF
Kd for $[Na^+]_{o(CLEFT)}$	8.70E+01 mM
Kd for $[Ca^{2+}]_{o(CLEFT)}$	1.30E+00 mM
$INaK_{pmp}$	
I_{max}	2.04E+00 μA/μF
Kd for $[Na^+]_{i(MYOPLASM)}$	1.00E+01 mM
Kd for $[K^+]_{o(CLEFT)}$	1.50E+00 mM

CALCULATION OF THE MEMBRANE POTENTIAL

The membrane potential was calculated by integrating of differential equation $d(V_m)/dt = -(\Sigma I_{ion} + I_{stim})/C_m$. Numerical integration was carried out according to the modified Euler's method published by Rudy at al[78]. Depending on the estimated error, the length of the instantaneous time step varied between 0.001 and 10 ms.

TABLE 7
CURRENT EQUATIONS

total mebrane currents

$$\sum I_{Na} = I_{Na} + I_{Bkg,Na} + 3 \cdot I_{NaCaEx} + 3 \cdot I_{NaKpmp}$$

$$\sum I_K = I_{to} + I_{Kur} + I_{Kr} + I_{Ks} + I_{K1} - 2 \cdot I_{NaKpmp}$$

$$\sum I_{Ca} = I_{CaT} + I_{CaL} + I_{Bkg,Ca} - 2 \cdot I_{NaCaEx}$$

$$\sum I_{Cl} = I_{Bkg,Cl}$$

intracellular ion concentrations except Ca^{2+}

$$M_z = 10^{-3} \cdot \frac{C_m \cdot A_{cap}}{z \cdot F \cdot VOL_{MYO}}$$

$$J_{m,X} = -M_{z_X} \cdot \sum I_X$$

$$[X]_{i,new} = [X]_{i,old} + \Delta t_{new} \cdot J_{m,X}$$

ion concentrations in the cleft - space

$$J_{cleft,X} = \frac{[X]_{bulk} - [X]_{cleft}}{\tau_{cleft}}$$

$$VOLR_{cleft}^{myo} = \frac{VOL_{myo}}{VOL_{cleft}}$$

$$[X]_{cleft,new} = [X]_{cleft,old} + (J_{cleft,X} - \Delta t_{new} \cdot J_{m,X} \cdot VOLR_{cleft}^{myo})$$

Ca^{2+} leak from network - SR

$$J_{NSR,leak} = IF\ ([Ca^{2+}]_{NSR} < [Ca^{2+}]_{myo})\ THEN\ 0\ ELSE\ \frac{[Ca^{2+}]_{NSR} - [Ca^{2+}]_{myo}}{\tau_{NSR,leak}}$$

Ca^{2+} uptake (SERCa)

$$J_{NSR,Up} = J_{NSR,UPmax} \cdot \frac{1}{1 + \frac{Kd_{Ca,NSR,Up}}{[Ca^{2+}]_{MYO}}}$$

intrareticular Ca^{2+} flow

$$J_{NSR,trans} = \frac{[Ca^{2+}]_{NSR} - [Ca^{2+}]_{JSR}}{\tau_{NSR,trans}}$$

Ca^{2+} concentration in network - SR

$$[Ca^{2+}]_{NSR,new} = [Ca^{2+}]_{NSR} + \Delta t \cdot (J_{NSR,Up} \cdot VOLR_{NSR}^{myo} - J_{NSR,leak} - J_{NSR,trans})$$

Ca^{2+} - induced Ca^{2+} release (CICR)

$$t_{CICR,new} = IF\ (-35mV < V_m)\ THEN\ t_{CICR} + \Delta t\ ELSE\ 0$$

$$CICR_{on} = \frac{1}{1 + exp(-\frac{t_{CICR} - 4}{5})}$$

$$CICR_{off} = 1 - CICR_{on}$$

$$CICR_{rel} = \frac{1}{1 + exp(\frac{\sum I_{Ca} + 5}{0.9})}$$

$$J_{CICR} = J_{CICR,max} \cdot CICR_{on} \cdot CICR_{off} \cdot CICR_{rel} \cdot ([Ca^{2+}]_{JSR} - [Ca^{2+}]_{myo})$$

Ca^{2+} overload - induced Ca^{2+} release

$$IF\ ([CaCSEQ]_{over,Thr} <= [CaCSEQ])\ AND\ (50\ ms < t_{over})\ THEN$$

$$t_{over,new} = 0,\ J_{over,max} = 4$$

$$ELSE$$

$$t_{over,new} = t_{over} + \Delta t,\ J_{over,max} = 0$$

$$OVER_{on} = 1 - exp(-\frac{t_{over}}{\tau_{over,on}})$$

$$OVER_{off} = exp(-\frac{t_{over}}{\tau_{over,off}})$$

$$J_{over} = J_{over,max} \cdot OVER_{on} \cdot OVER_{off} \cdot ([Ca^{2+}]_{JSR} - [Ca^{2+}]_{myo})$$

Ca^{2+} concentration in the junctional SR (JSR)

$$[Ca^{2+}]_{JSR,new} = \frac{-b + \sqrt{b^2 + 4c}}{2}$$

$$b = [CSEQ]_{total} - [CaCSEQ] - \Delta_{[Ca]JSR} - [Ca^{2+}]_{JSR} + Kd_{Ca,CSEQ}$$

$$c = Kd_{Ca,CSEQ} \cdot ([CaCSEQ] + \Delta_{[Ca]JSR} + [Ca^{2+}]_{JSR})$$

$$\Delta_{[Ca]JSR} = \Delta t \cdot (J_{NSR,trans} - J_{CICR} - J_{over})$$

$$[CaCSEQ] = [CSEQ]_{total} \cdot \frac{1}{1 + \frac{Kd_{Ca,CSEQ}}{[Ca^{2+}]_{JSR}}}$$

Ca^{2+} concentration in the myoplasm

$$[Ca^{2+}]_{myo,new} = \frac{2}{3}\sqrt{b^2 - 3 \cdot c} \cdot \cos\left(\frac{\arccos\left(\frac{9 \cdot b \cdot c - 2 \cdot b^3 - 27 \cdot d}{2 \cdot (b^3 - 3 \cdot c)^{3/2}}\right)}{3}\right) - \frac{b_2}{3}$$

$$A = Kd_{Ca,TROP} + Kd_{Ca,CALM}$$

$$b = [CALM]_{total} + [TROP]_{total} - [Ca^{2+}]_{total} + A$$

$$c = (Kd_{Ca,CALM} \cdot Kd_{Ca,TROP}) - [Ca^{2+}]_{total} \cdot A + [TROP]_{total} \cdot Kd_{Ca,CALM} + [CALM]_{total} \cdot Kd_{Ca,TROP}$$

$$d = -[Ca^{2+}]_{total} \cdot Kd_{Ca,CALM} \cdot Kd_{Ca,TROP}$$

$$[CaTROP] = [TROP]_{total} \frac{1}{1 + \frac{Kd_{Ca,TROP}}{[Ca^{2+}]_{myo}}}$$

$$[CaCALM] = [CALM]_{total} \frac{1}{1 + \frac{Kd_{Ca,CALM}}{[Ca^{2+}]_{myo}}}$$

$$[Ca^{2+}]_{total} = [CaTROP] + [CaCALM] + \Delta_{[Ca]myo} + [Ca^{2+}]_{myo}$$

$$\Delta_{[Ca]myo} = \Delta t \cdot (J_{m,Ca} + (J_{NSR,leak} - J_{NSR,Up}) \cdot VOLR_{myo}^{NSR} + (J_{CICR} + J_{OVER}) \cdot VOLR_{myo}^{JSR})$$

$Na^+ - Ca^{2+}$ exchanger

$$I_{NaCaEx} = I_{NaCaEx,max} \cdot f_{scale} \cdot f_{Na_o} \cdot f_{Ca_o} \frac{\exp(\gamma \frac{V_m \cdot F}{RT}) \cdot (\frac{[Na^+]_i}{[Na^+]_o})^3 - \exp((1-\gamma)\frac{V_m \cdot F}{RT}) \frac{[Ca^{2+}]_i}{[Ca^{2+}]_o}}{1 + k_{sat} \cdot \exp((1-\gamma)\frac{V_m \cdot F}{RT})}$$

$$f_{scale} = 200, \quad f_{Na_o} = \frac{1}{1 + (\frac{Kd_{Ex,Na_o}}{[Na^+]_o})^3}, \quad f_{Ca_o} = \frac{1}{1 + \frac{Kd_{Ex,Ca_o}}{[Ca^{2+}]_o}}, \quad \gamma = 0.35, \quad k_{sat} = 0.1$$

sarcolemmal $Na^+ - K^+$ pump

$$I_{NaKpmp} = I_{NaKpmp,max} \cdot f_{Na} \cdot f_K \cdot \frac{1}{1 + 0.1245 \cdot \exp(-0.1\frac{F \cdot V_m}{RT}) + 0.0052 \cdot \exp(-\frac{F \cdot V_m}{RT}) \cdot \sigma}$$

$$f_{Na} = \frac{1}{1 + (\frac{Kd_{NaK,Nai}}{[Na^+]_i})^2}, \quad f_K \frac{1}{1 + \frac{Kd_{NaK,Ko}}{[K^+]_o}}, \quad \sigma = \exp(\frac{[Na^+]_o}{67.3}) - 1$$

background currents

$$I_{Bkg,Na} = g_{Bkg,Na} \cdot (V_m - E_{Na})$$
$$I_{Bkg,Ca} = g_{Bkg,Ca} \cdot (V_m - E_{Ca})$$
$$I_{Bkg,Cl} = g_{Bkg,Cl} \cdot (V_m - E_{Cl})$$

$$E_X = \frac{RT}{z_x \cdot F} \ln(\frac{[X]_o}{[X]_i})$$

Equations for I_{Na} in general and as they were restructured for the human atrial AP-simulations

Lou-Rudy-equations

$$\tau_X = \frac{1}{X_\alpha + X_\beta}, \quad X_{ss} = X_\alpha \cdot \tau_X$$

$$I_{Na} = \overline{g_{Na}} \cdot m^3 \cdot h \cdot j \cdot (V_m - E_{Na})$$

$$E_{Na} = \frac{R \cdot T}{z \cdot F} \cdot \ln(\frac{[Na^+]_o}{[Na^+]_i})$$

$$x = x_{ss} - (x_{ss} - x) \cdot \exp(-\frac{t}{\tau_X})$$

$$m_\alpha = 0.32 \frac{V_m + 47.13}{1 - \exp(-\frac{V + 47.13}{10})}, \quad m_\beta = 0.08 \cdot \exp(-\frac{V_m}{11})$$

if $(V_m < -40\,mV)$ then:

$$h_\alpha = 0.135 \cdot \exp(-\frac{V_m + 80}{6.8})$$

$$h_\beta = 3.56 \cdot \exp(\frac{V_m}{12.65}) + 310000 \cdot \exp(\frac{V_m}{2.86})$$

$$j_\alpha = -(127140 \cdot \exp(\frac{V_m}{4.09}) + 0.00003474 \cdot \exp(-\frac{V_m}{22.77})) \cdot \frac{V_m + 37.78}{1 + \exp(\frac{V_m + 79.23}{3.22})}$$

$$j_\beta = 0.1212 \frac{\exp(\frac{V_m}{95.05})}{1 + \exp(-\frac{V_m + 40.14}{7.26})}$$

if $(-40\,mV < V_m)$ then:

$$h_\alpha = 0.0$$

$$h_\beta = 7.69 \frac{1}{1 + \exp(-\frac{V_m + 10.66}{11.1})}$$

$$j_\alpha = 0.0$$

$$j_\beta = 0.3 \frac{\exp(-\frac{V_m}{40000000})}{1 + \exp(-\frac{V_m + 32.0}{10})}$$

Restructured expressions

$$m_{ss} = \frac{1}{1 + \exp(\frac{V_m + 42.68}{-7.27})}$$

$$\tau_m = 0.005 + \frac{20.43}{1 + \exp(\frac{V_m + 292.24}{51.07}) + \exp(-\frac{V_m + 16.94}{7.26})}$$

$$h_{ss} = \frac{1}{1 + \exp(\frac{V_m + 66.53}{4.40})}$$

$$\tau_h = 0.137 + \frac{42.765}{1 + \exp(\frac{V_m + 55.64}{6.126}) + \exp(-\frac{V_m + 70.90}{5.56})}$$

$$j_{ss} = \frac{1}{1 + \exp(\frac{V_m + 66.41}{4.17})}$$

$$\tau_j = 3.32 + \frac{8208}{1 + \exp(\frac{V_m + 103.54}{8.95}) + \exp(-\frac{V_m + 40.86}{6.78})}$$

Gating functions of the sodium channel as they are given by the original LR-equations and by the iNa-model used for the AP-simulations presented

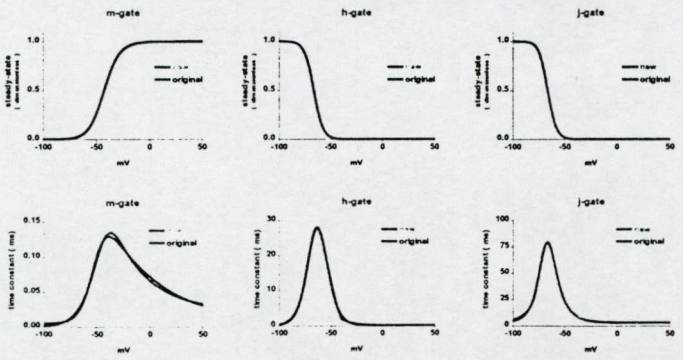

Equations for I_{CaL} in general and as they were restructured for the human atrial AP-simulations

Luo-Rudy-equations

$$x = x_{ss} - (x_{ss} - x)\cdot exp(-\frac{t}{\tau_x})$$

$$a_{ss} = \frac{1}{1+exp(-\frac{V_m+10}{6.24})}$$

$$\tau_a = a_{ss}\cdot\frac{1-exp(-\frac{V_m+10}{6.24})}{\frac{V_m+10}{28.57}}$$

$$b_{ss} = \frac{1}{1+exp(\frac{V_m+32}{8})} + 0.6\cdot\frac{1}{1+exp(-\frac{V_m-50}{20})}$$

$$\tau_b = \frac{1}{0.020+0.0197\cdot exp(-(\frac{V_m+10}{29.67})^2)}$$

$$bCa_{ss} = \frac{1}{1+\frac{[Ca^{2+}]}{0.00035}},$$

$$P_s = \overline{P_s}\cdot zF\frac{V_m\cdot z\,F}{RT}\cdot\frac{[S^{z+}]_i\cdot exp(\frac{V_m\cdot zF}{RT})-[S^{z+}]_o}{exp(\frac{V_m\cdot zF}{RT})-1},$$

and

$$iCaL_{Ca} = P_{Ca}\cdot a\cdot b\cdot bCa,$$
$$iCaL_{Na} = P_{Na}\cdot a\cdot b\cdot bCa,$$
$$iCaL_K = P_K\cdot a\cdot b\cdot bCa,$$

and

$$iCaL_{TOTAL} = iCaL_{Ca} + iCaL_{Na} + iCaL_K$$

Courtemanche-Nattel

as the LR-model, but

$$i_{CaL} = \overline{g_{CaL}}\cdot a\cdot b\cdot bCa\cdot(V_m - E_{Ca}),$$

$$E_{Ca} = \frac{RT}{z_{Ca}\cdot F}\cdot ln(\frac{[Ca^{2+}]_o}{[Ca^{2+}]_i}),$$

$$\tau_b = \frac{9}{0.020+0.0197\cdot exp(-(\frac{V_m+10}{29.67})^2)},$$

$$\tau_{bCa} = 2$$

Restructured expressions

$$a_{ss} = \frac{1}{1+exp(-\frac{V_m+10}{6.24})}$$

$$\tau_a = 0.317 + \frac{207.41}{1+exp(\frac{V_m+77}{16.96})+exp(-\frac{V_m-57}{16.9})}$$

$$b_{ss} = \frac{1}{1+exp(\frac{V_m+28.0}{6.9})}$$

$$\tau_b = 451.1 + \frac{245.0}{1+exp(\frac{V_m-19.3}{9.81})+exp(-\frac{V_m+39.3}{9.81})}$$

$$bCa_{ss} = \frac{1}{1+\frac{[Ca^{2+}]_i}{0.00035}}$$

$$\tau_{bCa} = 2$$

$$iCaL = \overline{g_{CaL}}\cdot a\cdot b\cdot bCa\cdot(V_m - E_{Ca})$$

Gating functions of the L-type calcium channel as they are given by the Courtemanceh-Nattel-equations and by the iCa_L-model used for atrial AP-simulations

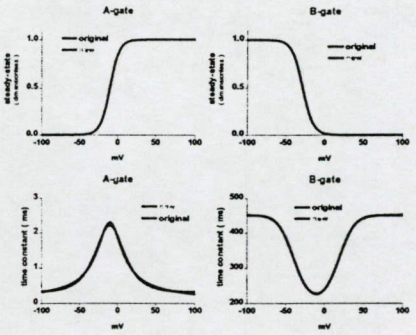

T-type Ca^{2+} current

$$I_{CaT} = g_{CaT}\cdot a^2\cdot b\cdot(V_m - E_{Ca})$$

$$\tau_a = 23.7 + 6.1\frac{1}{1+exp(\frac{V_m+25}{-14.5})}$$

$$a_{ss} = \frac{1}{1+exp(\frac{V_m+60}{-10.8})}$$

$$\tau_b = IF\ (V_m < 0)\ THEN\ 10 - 0.875\cdot V_m\ \ ELSE\ 10$$

$$b_{ss} = \frac{1}{1+exp(\frac{V_m+60}{5.6})}$$

transient outward K^+ current

$$I_{to1} = g_{ito1}\cdot a^3\cdot b\cdot(V_m - E_K)$$

$$\tau_a = \frac{1}{k_{Q10}(\alpha+\beta)}$$

$$k_{Q10} = 3,\quad \alpha = \frac{0.65}{exp(\frac{V_m+10}{-9.5})+exp(\frac{V_m-30}{-59})},\quad \beta = \frac{0.65}{2.5+exp(\frac{V_m+82}{17})}$$

$$a_{ss} = \frac{1}{1+exp(\frac{V_m+20.47}{-17.54})}$$

$$\tau_b = \frac{1}{k_{Q10}(\alpha+\beta)}$$

$$k_{Q10} = 3,\quad \alpha = \frac{1}{18.53+exp(\frac{V_m+113.7}{10.95})},\quad \beta = \frac{1}{35.56+exp(\frac{V_m+1.26}{-7.44})}$$

$$b_{ss} = \frac{1}{1+exp(\frac{V_m+43.1}{5.3})}$$

ultrarapid delayed rectifier K^+ current

$$I_{to1} = g_{max}\cdot f_{Vm}\cdot a^3\cdot b\cdot(V_m - E_K)$$

$$f_{Vm} = 1 + \frac{10}{1+exp(\frac{V_m-15}{-13})}$$

$$\tau_a = \frac{1}{k_{Q10}(\alpha+\beta)}$$

$$k_{Q10} = 3,\quad \alpha = \frac{0.65}{exp(\frac{V_m+10}{-8.5})+exp(\frac{V_m-30}{-59})},\quad \beta = \frac{0.65}{2.5+exp(\frac{V_m+82}{17})}$$

$$a_{ss} = \frac{1}{1+exp(\frac{V_m+10}{-9.6})}$$

$$\tau_b = \frac{1}{k_{Q10}(\alpha+\beta)}$$

$$k_{Q10} = 3,\quad \alpha = \frac{1}{21+exp(\frac{V_m-185}{28})},\quad \beta = exp(\frac{V_m-158}{16})$$

$$b_{ss} = \frac{1}{1+exp(\frac{V_m+99.45}{27.48})}$$

rapid component of the delayed rectifier K^+ current

$$I_{Kr} = g_{Kr} \cdot f_{Ko} \cdot f_{Vm} \cdot a \cdot (V_m - E_K)$$

$$f_{Ko} = \sqrt{\frac{[K^+]_o}{5.4}}, \quad f_{Vm} = \frac{1}{1 + \exp(\frac{V_m + 9}{22.4})}$$

$$\tau_a = \frac{1}{\alpha + \beta}$$

$$\alpha = \frac{0.00138 \cdot (V_m + 14.2)}{1 - \exp(\frac{V_m + 14.2}{-8.13})}, \quad \beta = \frac{0.00061 \cdot (V_m + 38.9)}{\exp(\frac{V_m + 38.9}{6.9}) - 1}$$

$$a_{SS} = \frac{1}{1 + \exp(\frac{V_m + 21.5}{-7.5})}$$

slow component of the delayed rectifier K^+ current

$$I_{Ks} = g_{Ks} \cdot f_{Ca_o} \cdot a^2 \cdot (V_m - E_K)$$

$$f_{Ca_o} = \frac{1}{1 + \frac{Kd_{iKs,Cao}}{[Ca^{2+}]_i}}$$

$$\tau_a = \frac{1}{k_{Q10} \cdot (\alpha + \beta)}$$

$$k_{Q10} = 2, \quad \alpha = \frac{0.000040 \cdot (V_m - 19.9)}{1 - \exp(\frac{V_m - 19.9}{-17.0})}, \quad \beta = \frac{0.000035 \cdot (V_m - 19.9)}{\exp(\frac{V_m - 19.9}{9}) - 1}$$

$$a_{SS} = \sqrt{\frac{1}{1 + \exp(\frac{V_m + 21.5}{-7.5})}}$$

inward rectifier K^+ current

$$I_{K1} = g_{K1} \cdot \frac{1}{1 + \exp(\frac{V_m + 70}{10.29})} (V_m - E_K)$$

acetylcholine-activated K^+ current

$$I_{K1} = g_{K1} \cdot \frac{1}{1 + (\frac{Kd_{ACh}}{[ACh]})^{0.5}} \cdot (0.3 + \frac{0.7}{1 + \exp(\frac{V_m + 59.53}{17.18})}) \cdot (V_m - E_K)$$

ACKNOWLEDGEMENTS

First of all I would like to pay reverence to Professor **Ottó Fehér**, MD, DSc, to my tutor during my student-years, whose animated lectures first gave me the impetus to do research in the physiological sciences.

I am very grateful to Professor **László Szekeres**, MD, DSc, for starting me on the scientific road. His unweawering logical reasoning, his relentless devotion to clearing up scientific problems and also his ingenuity in conductiong experiments of great scientific value, all remain illuminating examples to me for my whole life in the cardiovascular research.

I am very grateful to Professor **Julius Gy. Papp**, MD, DSc, member of the Hungarian Academy of Sciences, and Professor **Varró Andás**, MD, DSc, for their constant support and also for providing me with opportunity to work as researcher under their motivating auspices. They were the first ones, who enthusiastically inspired me to develop computer programs for signal evaluation.

I am very obliged to **László Latzkovits**, MD, DSc, who encouraged me to cut through some of the fog surrounding research work, and for helping me to master the laboratory techniques.

I am immensely indebted to **János Pataricza**, MD, PhD. Without teaming scientific discussions with him, I am sure I would never have had the heart to complete this thesis.

I am much obliged to Professor **Ursula Ravens**, MD, DSc. She has always trust me and gave me the opportunity to work on scientific questions connected with pathophysiology and pharmacology of atrial fibrillation. She is my model of what a good scientist should be like. *Ich bin bei Frau Professor Ravens zu ewigem Dank verpflichtet, für die Möglichkeit unter*

Ihrer gewissenhafter Aufsicht arbeiten und mit Ihr wissenschaftliche Themen besprechen zu können. Ihr Beispiel ist mir zum Weg, zum Leben und zur Wahrheit geworden, wodurch es Wissenschaft zu treiben allein ehrlich und einzig möglich ist.

I am most indebted to **Erich Wettwer**, MD, DSc, **Dobomir Dobrev**, MD, PhD, and **Torsten Christ**, MD, PhD for theirconstant support in my research work in Dresden and for the straightforward discussions, that opened me eyes to exciting new scientific horizons.

David Curley, PhD, and **Rimanóczy Ágnes**, PhD, are owed a debt of gratitude for their conscientious help in improving the English of this manuscript. The many hours they willingly sacrificed demands that their names be included here.

REFERENCES

[1] Pasty BM. Manolio TA, Kuller LH, Kronmal RA, Cushman M, Fried LP, White R, Furberg CD, Rautaharju PM. Incidence of and risk factors for atrial fibrillation in older adults. *Circulation.* 1997; 96:2455-2461.

[2] Tikanoja T, Kirkinen P, Nikolajev K, Eresmaa L, Haring, P. Familial atrial fibrillation with fetal onset. *Heart.* 1998; 79:195-197.

[3] Prystowsky E. Katz A. Atrial fibrillation. In Topol E (ed), *Textbook of Cardiovascular Medicine.* Philadelphia: Lipincott-Raven.1998; (pp. 1661-1693).

[4] Stewart S, Hart CL, Hole DJ, McMurray JJV. Population prevalence, incidence and predictors of atrial fibrillation in the Renfew/Paisley study. *Heart.* 2001; 86:516-521.

[5] Gibbs CR, Lip GYH, Benjamin EJ, Wolf PA, d'Agostino RB. Silberschatz H. Kannel WB, Levy D. Atrial fibrillation and ethnicity response. *Circulation.* 1999; 100:E151-153.

[6] Halperin JL, Hart RG. Atrial fibrillation and stroke: new ideas, persisting dilemmas. *Stroke.* 1988; 19:937-941.

[7] Wolf PA, Dawbwr TR, Thomas HE, Kannel WB. Epidemologic assesment chronic atrial fibrillation and risk of stroke: the Franingham study. *Neurology.* 1978; 28:973-941.

[8] Shih HT. Anatomy of the action potential in the heart. *Tex Heart Inst J.* 1994; 21(1):30-41.

[9] Gelband H, Bush HL, Rosen MR, Myerburg RJ, Hoffman BF. Electrophysiologic properties of isolated preparations of human atrial myocardium.*Circ Res.* 1972; 30(3):293-300.

[10] Hondeghem LM, Carlson L, Duker G. Instability and triangulation of the action potential predict serious proarrhythmia, but action potential prolongation is antiarrhythmic. *Circulation.* 2001; 103:2004-2013.

[11] Schneider M, Proebstle T, Hombach V, Hannekum A, Rudel R. Characterization of the sodium current in isolated human cardiomyocytes. *Pflügers Arch.* 1994; 428:84-90

[12] Li GR, Nattel S. Properties of human atrial I_{Ca} at physiological temperatures and relevance to action potential. *Am J. Physiol.* 1997; 272 (41):H227-H235.

[13] Nargeot J. A Tale of two (calcium) channels. *Circ Res.* 2000; 86:613-615.

[14] Lemaire S, Piot C, Seguin J, Nargeot J, Richard S. Tetrodotoxin-sensitive Ca^{2+} and Ba^{2+} currents in human atrial myocytes. *Receptors and Channels.* 1995; 3(2):71-81.

[15] Shorofsky SR, Balke CW. Calcium currents and arrhythmias: Insight from molecular biology. *Am J Med.* 2001; 280(5):1327-1339.

[16] Bernardeau A, Hatem SN, Rucker-Martin C, Le Grand B, Mace L, Dervanian P, Mercadier JJ, Coraboef E. Contribution of Na^+/Ca^{2+} exchange to action potential of human atrial myocytes. *Am J Physiol.* 1996; 27(3):1151-1161.

[17] Maier LS, Barckhausen P, Weisser J, Aleksic I, Baryalei M, Pieske. Ca^{2+} handling in isolated human atrial myocardium. *Am J Physiol.* 2000; 279(3):952-958.

[18] Bers DM. Calcium and cardiac rhythms. *Circ Res.* 2002; 90:14-17.

[19] Shibata EF, Drury T, Refsum H, Aldrete V, Giles. Contribution of a transient outward current to repolarization in human atrium. *Am J Physiol.* 1989; 257(6):1773-1781.

[20] Escande D, Coulombe A, Faivre F, Deroubaix E, Coraboef E. Two types of transient outward currents in adult human atrial cells. *Am J Physiol.* 1987; 252(21):142-148.

[21] Crumb WJ, Pigott JD, Clarkson CW. Comparison of I_{to} in young and adult human atrial myocytes: evidence for developmental changes. *Am J Physiol.* 1995; 268:1335-1342.

[22] Feng J, Xu D, Wang Z, Nattel S. Ultrarapid delayed rectifier current inactivation in human atrial myocytes: properties and consequences. *Am J Physiol.* 1998; 275(5):H1717-1725.

[23] Priori S, Barhanin J, Hauer RNW, Haverkamp W, Jongsma HJ, Kleber AG, McKenna WJ, Roden DM, Rudy Y, Schwartz K, Schwartz P, Towbin JA, Wilde AM. Genetic and molecular basis of cardiac arrhythmias: impact on clinical management. *Circulation.* 1999; 99:674-681.

[24] Barry DM, Nerbonne JM. Myocardial potassium channels: electrophysiological and molecular diversity. *Annu Rev Physiol.* 1996; 58:363-394.

[25] Wang Z, Fermi B, Nattel S. Rapid and slow components of delayed rectifier current in human atrial myocytes. *Cardiovasc Res.* 1994; 28(10):1540-1546.

[26] Bertaso F, Sharpe CC, Hendry BM, James AF. Expression of voltage gated K^+ channels in human atrium. *Basic Res Cardiol.* 2002; 97(6):424-433.

[27] Koumi S, Backer CL, Arentzen CE. Characterization of inwardly rectifying K^+ channel in human cardiac myocytes. *Circulation.* 1995; 92:164-174.

[28] Firek L, Giles WR. Outward currents underlying repolarization in human atrial myocytes. *Cardiovasc Res.* 1995; 30(1):31-38.

[29] McDongough AA, Velotta JB, Schwingler RH, Philipson KD, Farley RA. The cardiac sodium pump: structure and function. *Basic Res Cardiol.* 2002; 97(Suppl 1):19-24.

[30] Borchard U, Hafner D. Ion channels and arrhythmias. *Z Kardiol.* 2000; 89(suppl 3):6-12.

[31] Heidbuchel H, Vereecke J, Carmeliet E. Three different potassium channels in human atrium. Contribution to the basal potassium conductance. *Circ Res.* 1990; 66(5):1277-1286.

[32] Roden DM, Balser JR, George AL. Anderson ME. Cardiac ion channels. *Ann Rev Physiol.* 2002; 64:431-475.

[33] Biel M, Schneider A, Wahl C. Cardiac HCN channels: structure, function and modulation. *Trends Cardiovasc Med.* 2002; 15(5):206-212.

[34] Kamalvand K, Tan K, Lloyd G, Gill J, Bucknall C, Sulke N. Alterations in atrial electrophysiology associated with chronic atrial fibrillation in man. *Eur Heart J.* 1999; 20(12):856-857.

[35] Libbus I, Rosenbaum DS. Remodelling of cardiac repolarization: mechanisms and implications of remodelling. *Card Electrophysiol Rev.* 2002; 6(3):302-310.

[36] Nattel S, Li D, Yue L. Basic mechanisms of atrial fibrillation: very new insights into very old ideas. *Annu Rev Physiol.* 2000; 62:51-77.

[37] Gaspo R, Bosch R, Talajic M, Nattel S. Functional mechanisms underlying tachycardia-induced sustained atrial fibrillation in a chronic dog model. *Circulation.* 1997;96:4027-4035

[38] Zipes, DP. Atrial fibrillation. A tachycardia-induced atrial cardiomyopathy. *Circulation.* 1997; 95:562-564.

[39] Roithinger FX, Lesh. What is the relationship of atrial flutter and fibrillation. *Pacing Clin Electrophysiol.* 1999; 22(4): 643-654.

[40] Cao JM; Qu Z, Kim YH, Wu TJ, Garfinkel A, Weiss JN, Karagueuzian HS, Chen PS. Spatiotemporal heterogeneity in the induction of ventricular fibrillation by rapid pacing.(Importance of cardiac restitution properties) *Circ Res.* 1999;84:1318-1331

[41] Nattel S. Ionic remodelling in the heart: pathophysiological significance and new therapeutic opportunities for atrial fibrillation. *Circ Res.* 2000; 87(16):440-447.

[42] ACC/AHA/ESC guidelines for management of patients with atrial fibrillation. *Circulation.* 2001; 104:2118-2150.

[43] Bosch RF, Zeng X, Grammer JB, Popovic, Maewis C, Kühlkamp V. Ionic mechanisms of electrical remodelling in human atrial fibrillation. *Cardiovasc Res.* 1999; 44(1): 121-131.

[44] Van Wagoner DR, Nerbonne JM. Molecular basis of electrical remodelling in atrial fibrillation. *J Mol Cell Cardiol.* 2000; 32(6): 1101-1107.

[45] Ehrlich JR, Nattel S, Hohnloser SH. Atrial fibrillation and congestive heart failure: specific considerations at the intersection of two common and important disease sets. *J Cardiovasc Electrophysiol.* 2002; 13(4):399-405.

[46] Swyngehdauw B. Molecular mechanisms of myocardial remodelling. *Physiol Rev.* 1999; 79:215-262.

[47] Wijffels MCEF, Kirchhof CJHJ, Dorland R, Allessie MA. Atrial fibrillation begets atrial fibrillation. *Circulation.* 1995; 92:1954-1968.

[48] Sing BN, Mody FV, Lopez B, Sarma JS. Antiarrhythmic agents for atrial fibrillation: focus on prolonging atrial repolarization. *Am J Cardiol.* 1999; 84(9A):161R-173R.

[49] Van Gelder IC, Tuinenburg AE, Schoonderwoerd BS, Tielman RG, Crijns HJ. Pharmacologic versus direct-current electrical cardioconversion of atrial flutter and fibrillation. *Am J Cardiol.* 1999; 84(9A):147R-151R.

[50] Levy S. Pharmacologic management of atrial fibrillation: current therapeutic strategies. *Am Heart J.* 2001; 141(2 Suppl):S15-S2.

[51] Anderson JL, Prystowsky EN. Sotalol: An important new antiarrhythmic. *Am Heart J.* 1999; 137(3):388-409.

[52] Murray, K. T. Ibutilide. *Circulation.* 1998; 97: 493-497.

[53] Sing BN. Current antiarrhythmic drugs: An overwiev of mechanisms of action and potential clinical utility. *Cardiovasc Electrophysiol.* 1999; 10(2):283-301.

[54] Karam R, Marcello S, Brooks RR, Corey AE, Moore A. Azimilide dihydrochloride, a novel antiarrhythmic agent. *Am J Cardiol.* 1998; 81(6A):40D-46D.

[55] Ayers GM, Rho TH, Ben-David J, Besch HR, Zipes DP. Amiodarone instilled into the canine pericardial sac migrates transmurally to produce electrophysiologic effects and suppress atrial fibrillation. *J Cardiovasc Electrophysiol.* 1996; 7:713-721.

[56] Capucci A, Villani GQ, Aschieri D, Rosi A, Piepoli MF. Oral amiodarone increases the efficacy of direct-current cardioversion in restoration of sinus rhythm in patients with chronic atrial fibrillation. *Eur Heart J.* 2000; 21(1):66-73; Comment in: *Eur Heart J.* 2000; 21(1):11-2

[57] Vaughan Williams EM. Classifying antiarrhythmic actions: by facts or speculations. *J Clin Pharmacol. 1992;* 32(11):964-977.

[58] Nattel S, Singh BN. Evolution, machanism, and classification of antiarrhythmic drugs: focus on Class 3 actions. *Am J Cardiol.* 1999; 84(9A):11R-19R.

[59] Weirich J, Wenzel W. Current classification of antiarrhythmic agents. *Z Kardiol.* 2000; 89 (suppl 3):62-67.

[60] Lee SH, Yu WC, Cheng JJ, Hung CR, Ding YA, Chang MS, Chen SA. Effect of verapamil on long-term tachycardia-induced atrial electrical remodelling. *Circulation.* 2000; 101:200-206

[61] Bertaglia E, d'Este D, Zanocco A, Zerbo F, Pascotto P. Effects of pretreatment with verapamil on early recurrences after electrical cardioversion of persistent atrial fibrillation: a randomised study. Br. *Heart J.* 2001; 85:578-580

[62] Villani GQ, Piepoli MF, Terracciano C, Capucci A. Effects of diltiazem pretreatment on direct-current cardioversion in patients with persistent atrial fibrillation: A single-blind, randomized, controlled study. *Am Heart J.* 2000; 140(3):437-43

[63] Cardiac Arrhythmia Supression Trial (**CAST**) Investigators. Effect of encainide and flecainide on mortality in a randomised trial of arrhythmia supression after myocardial infarction. *N Engl J Med.* 1989; 321: 406-412

[64] Waldo AL, Camm AJ, deRuyter H, Friedman PL, McNeil DJ, Paulus JF, Pitt B, Pratt CM, Schwarz PJ, Veltri EP. Effect of d-sotalol on mortality in patients with left ventricular dysfunction after recent and remote myocardial infarction. *Lancet.* 1996;348:7-12

[65] Van Gelder IC, Brugemann J, Crijns HJ. Current treatment recommendations in antiarrhythmic therapy. *Drugs.* 1998; 55(3): 331-346.

[66] Fedida D, Wible B, Wang Z, Fermini B, Faust F, Nattel S, Brown R. Identity of a novel delayed rectifier current from human heart with a cloned channel current. *Circ Res.* 1993. 73(1):210-206.

[67] Feng J, Wible B, Li GR, Wang Z, Nattel S. Antisense oligonucleotides directed against Kv1.5 mRNA specifically inhibit ultrarapid delayed rectifier K+ current in cultured human atrial myocytes. *Circ Res.* 1997; 80:572-579.

[68] London B, Guo W, Lee JS, Shusterman V, Rocco CJ, Logothetis DE, Nerbonne JM, Hill JA. Targeted replacement of Kv1.5 in the mouse leads to loss of the 4-aminopyridine-sensitive component of iK_{slow} and resistance to drug-induced QT-prolongation. *Circ Res.* 2001; 88:940-946.

[69] Escande D, Loisance D, Planche C, Coraboeuf E. Age-related changes of action potential plateau shape in isolated human atrial fibers. *Am J Physiol.* 1985; 249(4): 843-850.

[70] Escande D, Coraboeuf E, Planche C, Lacour-Gayet F. Effects of potassium conductance inhibitors on spontaneous diastolic depolarization and abnormal automaticity in human atrial fibers. *Basic Res Cardiol.* 1986; 81(3):244-257.

[71] Courtemanche M, Ramirez JR, Nattel S. Ionic mechanisms underlying human atrial action potential properties: insight from a mathematical model. *Am J Physiol.* 1998; 275(44):301-321.

[72] Németh M, Virág L, Hála O, Varró A, Kovács G, Thormählen D, Papp JGy. The cellular electrophysiological effects of tedisamil in human atrial and ventricular fibers. *Cardiovasc Res.* 1996; 31:246-258.

[73] Dobrev D, Graf EM, Wettwer E, Himmel HM, Hála O, Doerfel C, Christ T, Schüler S, Ravens U. Molecular basis of downregulation of G-protein-coupled inward rectifying K^+ current (IKACh) in chronic human atrial fibrillation. Decrease in GIRK mRNA correlates with reduced IKACh and muscarinic receptor-mediated shortening of action potentials. *Circulation.* 2001; 104:2551-2557.

[74] Ramirez RJ, Nattel S, Courtemanche M. Mathematical analysis of canine atrial action potentials: rate, regional factors and electrical remodelling. *Am J Physiol.* 2000; 279:1767-1758.

[75] Nygren A, Fiset C, Firek L, Lindblad DS, Clark RB, Giles. Mathematical model of an adult human atrial cell: The role of K^+ currents in repolarization. *Circ Res.* 1998; 82:63-81.

[76] Dokos S, Celler B, Lovell N. Ion currents underlying sinoatrial node pacemaker activity: A new single cell mathematical model. *J Theor Biol.* 1996; 181:245-273.

[77] Zeng J, Laurita KR, Rosenbaum DS, Rudy Y. Two components of the delayed rectifier K^+ current in ventricular myocytes of the guinea-pig type. *Circ Res.* 1995; 77:140-152.

[78] Luo CH, Rudy Y. A dynamic model of the cardiac ventricular action potential. I. Simulations of ionic currents and concentration changes. *Circ Res.* 1994; 74:1071-1096.

[79] Faber GM, Rudy Y. Action potential and contractility changes in $[Na^+]_i$ overloaded cardiac myocytes: A simulation study. *Biophys J.* 2000; 78:2392-2404.

[80] Kneller J, Ramirez RJ, Chaertier D, Courtemanche M, Nattel S. Time-dependent transients in an ionically based mathematical model of the canine atrial action potential. *Am J Physiol.* 2002; 282:1437-1451.

[81] Kneller J, Zou R, Vigmond EJ, Wang Z, Leon JL, Nattel S. Cholinergic atrial fibrillation in a computer model of a two-dimensional sheet of canine atrial cells with realistic ionic properties. *Circ Res.* 2002; 90: 1328-1353.

[82] Hála O, Wettwer E, Dobrev D, Christ T, Papp JGy, Ravens U. Selective outward current block with low concentration of 4-aminopyridine reveals a prominent role of IK_{ur} in determining the action potential plateau shape of human atrial tissue. *Circulation.* 2001; 104(17 Suppl II): P1328

[83] Hála O, Németh M, Varró A, Papp JGy. Electrophysiological effects of detajmium on isolated dog cardiac ventricular Purkinje fibers. *J Cardiovasc Pharmacol.* 1994; 24:559-565.

[84] Papp JGy, Miklós N, Krassói I, Mester L, Hála O, Varró A. Differential effects of chronically administered amiodarone on canine purkinje versus ventricular muscle. *J Cardiovasc Pharmacol Therapeut.*1996; 1(4):287-296.

[85] Németh M, Varró A, Virág L, Hála O, Thormälen D, Papp JGy. Frequency-dependent cardiac effects of tedisamil: comparison with quinidine and sotalol. *J Cardiovasc Pharmacol Therapeut.* 1997; 2(4):273-284.

[86] Varró A, Takács J, Németh M, Hála O, Virág L, Iost N, Baláti B, Agoston M, Vereckei A, Pastor G, Delbruyere M, Gautier P, Nisato D, Papp JGy. Electrophysiological effects of dronedarone (SR 33589), a noniodinated amiodarone derivative in the canine heart: comarison with amiodarone. *Br J Pharmacol.* 2001; 133(5):625-634.

[87] Németh M, Virág L, Hála O, Varró A, Kovács G, Thormählen D, Papp JGy. The cellular electrophysiological effects of tedisamil in human atrial and ventricular fibers. *Cardiovascular Res.* 1996; 31:246-248.

[88] Guillemare E, Marion A, Nisato D, Gautier P. Inhibitory effects of dronedarone on muscarinic K^+ current in guinea pig atrial cells. *J Cardiovasc Pharmacol.* 2000;36(6):802-805

[89] Moe GK, Rheinboldt WC, Abildskov JA. A computer model of atrial fibrillation. *Am Heart J.* 1964; 67:200-20

[90] Allessie MA, Lammers WJEP, Bonke FIM, Hollen J. Experimental evaluation of Moe's multiple wavelet hypothesis of atrial fibrillation. In Zipes DP, Jalife J, eds. *Cardiac Arrhythmias.* New York: Grune & Stratton; 1985: 265-276

[91] Cabo C, Pertsov AV, Salomonsz JR, Baxter W, Jalife J. Wave-front curvature as a cause of slow conduction and block in isolated cardiac muscle. *Circ Res.* 1994; 75:1014-1028

[92] Krinsky VI. Spread of excitation in an inhomogenous medium. *Biophysica* (USSR), 1966:11:776-784.

[93] Winfree AT. *When time breaks down.* Princeton, NJ: Princeton University Press; 1987.

[94] Karma A. Electrical alternans and spiral wave break up in cardiac tissue. *Chaos.* 1994; 4:461-472

[95] Panfilov AV, Hogweg P. Scroll break up in a three-dimensional excitable medium. *Physiol Rev E.* 1996; 53:1740-1743

[96] Courtemanche M, Winfree AT. Reentrant rotating waves in a Beeler-Reuter based model of two-dimensional cardiac electrical activity. *Int J Bifurc Chaos.* 1991; 1:431-444

[97] Efimov IR, Krinsky VI, Jalife J: Dynamics of rotating vortices in the Beeler-Reuter model of cardiac tissue. *Chaos Solitons Fractals.* 1995;5:531-526.

[98] Gray RA, Jalife J, Panfilov AV, Baxter WT, Cabo C, Davidenko JM, Pertsov AM. Mechanism of cardiac fibrillation. *Science.* 1995;270: 1222-1223

[99] Moe GK, Rheinboldt, Abildshov JA. A computer model of atrial fibrillation. *Am Heart J.* 1964;67:200-220.

[100] Frame LH, Simson MB. Oscillations of conduction, action potential duration, and refractoriness: a mechanism of spontaneous termination of reentrant tachycardias. *Circulation.* 1988; 78:1277-1287

[101] Weiss JN, Garfinkel A, Karagueuzian HS, Qu Z, Chen PS, MD. Chaos and the transition to ventricular fibrillation (A new approach to antiarrhythmic drug evaluation) *Circulation.* 1999;99:2819-2826.

[102] Riccio M, Koller M, Gilmour RF. Electrical restitution and spatiotemporal organization during ventricular fibrillation. *Circ Res.* 1999; 84:955-963

[103] Garfinkel A, Kim Y, Voroshilovsky O, Qu Z, Kil JR, Lee MY, Karagueuzian HS, Weiss JN, Chen PS. Preventing ventricular fibrillation by flattening cardiac restitution. *Proc Natl Acad Sci USA.* 2000; 97:6061-6066

[104] Nearing BD, Huang AH, Verrier RL. Dynamic tracking of cardiac vulnerability by complex demodulation of the T wave. *Science.* 1991; 252:437-440

[105] Kim BS, Kim YH, Hwang GS, Pak HN, Lee SC, Shim WJ, Oh DJ, Ro YM. Action potential duration restitution kinetics in human atrial fibrillation. *Am J Cardiol.* 39(8):1329-1336.

[106] Berridge MJ, Lipp P, Bootman. Nature Reviews. *Mol Cell Biol.* 2000; 1:11-21.

[107] Tieleman RG, Blaauw Y, Van Gelder IC, DeLangen CD, Grandjean JG, Patberg KW, Bel KJ, Allessie MA, Crijns HJ. Digoxin delays recovery from thachycardia-induced electrical remodelling of the atria. *Circulation.* 1999; 100(26):1836-1842.

[108] Leistad E, Aksnes G, Verburg E, Christensen G. Atrial contractile dysfunction after short-term atrial fibrillation is reduced by verapamil, but increased by Bay K8644. *Circulation.* 1996; 93:1747-1754.

[109] Dynkin EB. Die Grundlagen der Theorie der Markoffschen Processe in Gammel R, Heinz E, Hirzenbruch F, Hopf E, Hopf H. Maak W, Magnus W, Schmift FK, Stein K. Van der Waerden BL (Eds). *Die Grundlagen der mathematischen Wissenschaften in Einzeldarstellungen mit besonderer Berücksichtigung der Anwendungsgebiete.* Band 108. Berlin, Göttingen, Heidelberg. Springer Verlag. 1961.

[110] Hodgkin AL, Huxley AF. A quantitative description of mebrane current and its application to conduction and excitation in nerve. *J. Physiol. (Lond).* 1952; 117:500-544.

[111] Zagotta WN, Hoshi T, Aldrich RW. Shaker potassiom channel gating. III. Evaluation of kinetic models for activation. *J. Gen. Physiol.* 1994. 103:321-362.

[112] Schoppa NE, Sigworth FJ. Activation of Shaker potassium channels. III. An activation gating model for wild type and V2 mutant channels. J. *Gen. Phys.* 1998. 111:313-342.

[113] Eyring H, Lumry R, Woodbury JW. Some application of modern rate theory to physiological systems. *Rec Chem Prog.* 1949; 10:100-114.

[114] Sigg D, Qian H, Bezanilla F. Kramer's diffusion theory applied to gating kinetics of voltage-dependent ion channels. *Biophys J.* 1999; 76:782-803.